ARL-TR-8929 ● MAR 2020

DEVCOM ARMY RESEARCH LABORATORY

Properties and Protection of Wrought ZW3 and ZK60A Mg-Zn-Zr Magnesium Alloys

by John F Chinella

NOTICES

Disclaimers

The findings in this report are not to be construed as an official Department of the Army position unless so designated by other authorized documents.

Citation of manufacturer's or trade names does not constitute an official endorsement or approval of the use thereof.

Destroy this report when it is no longer needed. Do not return it to the originator.

ARL-TR-8929 ● MAR 2020

Properties and Protection of Wrought ZW3 and ZK60A Mg-Zn-Zr Magnesium Alloys

John F Chinella
Weapons and Materials Research Directorate, CCDC Army Research Laboratory

REPORT DOCUMENTATION PAGE

Form Approved
OMB No. 0704-0188

1. REPORT DATE *(DD-MM-YYYY)*	2. REPORT TYPE	3. DATES COVERED (From - To)
March 2020	Technical Report	November 15, 2013 – October 20, 2016

4. TITLE AND SUBTITLE
Properties and Protection of Wrought ZW3 and ZK60A Mg-Zn-Zr Magnesium Alloys

5a. CONTRACT NUMBER
W911QX-14-P-0481

5b. GRANT NUMBER

5c. PROGRAM ELEMENT NUMBER

6. AUTHOR(S)
John F Chinella

5d. PROJECT NUMBER

5e. TASK NUMBER

5f. WORK UNIT NUMBER

7. PERFORMING ORGANIZATION NAME(S) AND ADDRESS(ES)
CCDC Army Research Laboratory
ATTN: FCDD-RLW-MF
Aberdeen Proving Ground, MD 21005

8. PERFORMING ORGANIZATION REPORT NUMBER
ARL-TR-8929

9. SPONSORING/MONITORING AGENCY NAME(S) AND ADDRESS(ES)

10. SPONSOR/MONITOR'S ACRONYM(S)

11. SPONSOR/MONITOR'S REPORT NUMBER(S)

12. DISTRIBUTION/AVAILABILITY STATEMENT
Approved for public release; distribution is unlimited.

13. SUPPLEMENTARY NOTES
ORCID ID(s): Author, 0000-0002-2959-1794

14. ABSTRACT

This report characterizes microstructure, Charpy impact toughness, tensile properties, ballistic V50 protection, and failure (fracture) modes of magnesium-zinc-zirconium (Mg-Zn-Zr) alloys ZK60A-T5 (Mg-6.0Zn-0.45Zr) and ZW3 (Mg-3.0Zn-0.6Zr) ZK30. ZK60A-T5 and ZW3 flat profiles were extruded to thicknesses 25.4 mm, 38.1 mm, and 50.8 mm, 254 mm width, under respective specifications ASTM B 107B-13 and BS 2L 505. The ZW3 and ZK60A-T5 failure modes and material properties are characterized with microstructure, fracture features, and Charpy instrumented test (IT) measurements of force, energy, displacement, and time. Mechanical tests in tension demonstrate properties of strength and ductility and flow curves. True stress versus true strain properties and flow curves reveal strength, ductility, and power-law hardening. The Charpy IT shows the ductile displacement and fracture, the unstable crack fracture modes, and duration time period for non-catastrophic fracture by plastic displacement. V50 tests reveal protection levels and failure modes versus the 0.30-cal. APM2 projectile and 0.50-cal. fragment-simulating projectile (FSP). Areal density (AD) – V50 plots compare the ballistic protection performances to Mg AZ31-H24, WE43-T5, Mg-13Li-6Al, and aluminum (Al) 5083, 7039, 7020-T651, and 7017 protection materials. Charpy IT results of un-notched ZW3 specimens demonstrate excellent Mg toughness in force-displacement and duration of force-time, better than AM50 (Mg-Al-Mn) crash protection alloy. The 0.30-cal. APM2 V50 protection meets or exceeds 5083 Al and AZ31 Mg levels; 0.50-cal. FSP protection exceeds the AZ31B Mg, and 5083 Al levels up to 64 kg/m^2 AD. High tensile-ductility properties of ZW3 suggest capability to roll plate and to mitigate anisotropy effects in plate shapes.

15. SUBJECT TERMS
wrought magnesium, microstructure, mechanical properties, ZK60, ZW3, ZK30, ballistic protection

16. SECURITY CLASSIFICATION OF:			17. LIMITATION OF ABSTRACT	18. NUMBER OF PAGES	19a. NAME OF RESPONSIBLE PERSON
a. REPORT	b. ABSTRACT	c. THIS PAGE			John F Chinella
Unclassified	Unclassified	Unclassified	UU	64	19b. TELEPHONE NUMBER (Include area code) (410) 306-0866

Standard Form 298 (Rev. 8/98)
Prescribed by ANSI Std. Z39.18

Contents

List of Figures

List of Tables

Acknowledgments

Gratitude is expressed to Mr Bill Warfield, Extrusions Manager – Magnesium Elektron North America Incorporated, and Magnesium Elektron UK, for assistance and cooperation in procurement and fabrication of extrusion dies and custom-extrusion of flat profile shapes of magnesium alloys ZW3 and ZK60A-T5. Recognition and thanks is expressed to Mr David Gray, CCDC Army Research Laboratory, for cooperation and performance of mechanical tests in tension, and tension test data collection.

1. Introduction

This report demonstrates and characterizes microstructure, Charpy impact toughness, mechanical properties in tension, specific properties, and the ballistic V50 protection levels and fracture modes of the high-strength ductile wrought ZK60A-T5 (6.0 Zn–0.45 Zr)[1–6] and ZW3[*1,3,7] (3.0 Zn–0.6 Zr)[4] ZK30 type Mg alloys. Extrusion dies[†] of flat profiles were first designed and manufactured in three thicknesses of 25.4 mm, 38.1 mm, and 50.8 mm, each 254 mm in width with edges of full-thickness radius, which were employed in extrusion of ZK60A-T5 and ZW3 profiles of near equivalent dimensions under respective specifications ASTM B 107B-13[5] and BS 2L 505: March 1973.[7] To demonstrate the wrought ZW3 and ZK60A-T5 fracture modes and material properties, test material characterizations present hardness, microstructure, fracture features, and Charpy impact energy and instrumented test (IT) force, energy, displacement, and time.[8] Mechanical properties in tension demonstrate properties of strength and ductility and the engineering stress versus strain flow curves. True stress versus true strain properties and flow curves reveal strength, ductility, and power-law hardening.[9] The Charpy IT on un-notched (UN) 10 × 10-mm specimens reveal the approximate forces, displacement, and ductile fracture, the unstable crack fracture modes, and duration time period for non-catastrophic ductile fracture and displacement. Ballistic V50[10,11] tests reveal protection levels and failure modes versus the 0.30-cal. APM2 projectile and 0.50-cal. fragment-simulating projectile (FSP). Areal density (AD) – V50 regression plots compare the ballistic protection performance to Mg AZ31-H24,[12] WE43-T5,[13] Mg-13Li-6Al,[14] and the Al 5083,[15] 7039,[15,16] 7020-T651,[16] and 7017[17] protection materials. UN Charpy ITs of the ZW3 alloy demonstrate excellent Mg toughness of ductile displacement with equal time duration, 1.6× to 1.7× greater maximum force than AM50 (Mg-Al-Mn) crash protection alloy. The 0.30-cal. APM2 V50 protection meets or exceeds 5083 Al and AZ31 Mg levels; 0.50-cal. FSP protection exceeds the AZ31B Mg, and 5083 Al levels up to 64 kg/m^2 AD.

[*] Magnesium Elektron Limited, Manchester, England, Elektron wrought alloy.

[†] Drawings, date 02/14/14: 1) No. ME-100, part no. 1.0-inch × 10-inch bar, form factor 2, area 9.7854, square inch (6,313 mm^2), perimeter 21.142 inches; 2) No. ME-101, part no. 1.5-inch × 10-inch bar, form factor 1, area 14.5171, square inch (9,366 mm^2), perimeter 21.712 inches; 3) No. ME-102, part no. 2-inch × 10-inch bar, form factor 1, area 19.1416, square inch (12,349 mm^2), perimeter 22.283 inches.

2. Background

2.1 Outstanding Advantages of Magnesium Lightweight Materials and Structures

Density of material structure is most important for structural weight savings with a 1:1 return; and importantly, with vehicle weight saving there is a 50% return in fuel savings, which is secondary only to the 1:1 return from powertrain operation efficiency.[2] The Mg alloys are of current interest as commercial grade construction and component material largely for their material characteristics of the lowest metal 1.738 g/cm^3 density, high structural specific stiffness and high specific strength, which may be used for advantage for weight and fuel savings (e.g., with vehicle and aerospace components, high-speed precision-robotics, and portable structures).[2,3] Exploitation of the low density and specific properties are important factors in successful use. Further advantages are excellent castability and machinability, and weldability under controlled conditions. With concern to finite quantities of material resources of engineering structural metals, the Mg content of seawater is 0.13%, which provides near unlimited reserves. From the Great Salt Lake, Utah, U.S. Magnesium produces around 14% of world production of Mg with beneficial site accompaniment of product chemicals and minerals. China produces around 80% of the world's Mg. Good resistance to corrosion may be achieved for specific applications (e.g., in distilled water, solutions of sodium hydroxide, potassium hydroxide, alkaline media with p-H > 8.5, some ammonia compounds, and pure hydrofluoric acid). With control of manufacturing processes, control of purity levels from Fe, Ni, Cu, and by microalloying with Mn,[2] optimal corrosion performance may be achieved with performance consistent and competitive with die cast automotive aluminum alloys. Compared to polymers or polymer composites, Mg has better mechanical properties, resistance to aging and deterioration, electrical and thermal conductivity, electro-magnetic shielding, and constituents and volatiles of low toxicity;[2,3] the constituents, Mg, Zn, Mn, Ca, and Cu are vital to biological life. With concern to fire safety, the environment-dependent ignition temperature of specific high temperature Mg alloys, 590 °C to 1,107 °C, exceeds the thermal decomposition and ignition temperatures of often-toxic polymer materials.[18] Mg and metals have economics of commercial recycle-resale capability; Mg or metals may be compacted or section-cut for low cost recycle transport without great loss of product quality and value, unlike composite fiber of large structures. To attain high-end material microstructure advantages scaled to product, there is no paramount need for time consuming, costly layer-by-layer placement and debulking to avoid critical structural flaws that may lead to low impact toughness, localization of stress, delamination and onset of crack

fracture. As a structural metal, Mg now ranks third in production behind steel and aluminum. However, the use of Mg, 1999, primarily is in applications of alloying of aluminum alloys at 43%, the desulfurization of steel at 11%, and die casting at 36%.[2] The die casting is largely AZ91 (Mg-9.5Al-0.5Zn-0.3Mn) for demands of weight saving environment-friendly cars. Of the die casting alloys, the good ductility and energy absorbing AM series alloy segment (e.g., AM50 Mg-5Al-0.5Mn), is the fastest growing for application to lightweight automobile components subjected to deformation during a crash (e.g., seats, door, steering wheel, instrument panel).[2]

2.2 Disadvantages of Magnesium Alloys

Disadvantages of magnesium alloys are: low elastic modulus; limited cold workability and toughness due to limited plastic dislocation slip systems of the hexagonal close packed (HCP) Mg crystallographic lattice; limited strength and creep resistance at high temperatures; in wrought alloys yield strength asymmetry for the load modes of tensile and compression, and directional anisotropy of mechanical properties,[2,19] high levels of shrinkage during solidification which promotes porosity; high chemical reactivity which affects melting, processing, wrought work, and recycling; and limited resistance to corrosion which is cited as a maintenance interval shortcoming for aerospace structural applications.[2,3] The level of fracture toughness for onset of fracture by a sharp crack is low compared to aluminum or steel alloys.[2] Presumably rapid onset of surface corrosion of any primary structure may lead to pitting and initiation of stress corrosion or fatigue failure. The electromotive force of magnesium $Mg^{2+} + 2e^- \leftrightarrow Mg$, is –2.37 V;[2] only Na, Ca, K, and Li have more negative emf. Unlike Al or Ti, the passivation layer of surface oxide for Mg does not greatly protect from corrosion or adjust the emf potential. Therefore, Mg is by far the most anodic structural metal and galvanic coupling must be avoided. Mg is low in corrosion resistance to mineral acids, seawater, halogen salts, and sulphur compounds. Improved resistance to general corrosion for bare metal or surface treatment may be attained with high levels of metal purity by excluding Ni, Fe, and Cu as with the Mg alloys of ASTM grade D and especially the highest purity E-grade. However; the high purity levels may not be attained from specific product generation American Society of Testing Materials (ASTM) grades (e.g., A, B, C, specific ores, or some electrolytic production or recycling methods),[2,3] and in service, the environment can be a source of contact impurities. The advantage of high alloy purity to achieve improved resistance to general corrosion is somewhat of a disadvantage for recycling. There is a history of metal-production technical and developmental problems (e.g., feedstock and product purity, plant efficiency, environmental problems and social conflicts, high

start and operating financial costs, and demands of market pricing).[2] Hot extrusion and wrought work rate of Mg alloys may be limited in speed, and furthermore there may be less optimal effects of directional texture which may affect relatively low levels of failure strain; therefore, the most direct economic process may be casting.[2,3] The amount of eutectic forming constituents for cast alloys is low compared to Al. The Mg alloys that perform mold-feed well in cast manufacture are those that form eutectic phase; either by Mg-Al non-equilibrium solidification, or zirconium rare earth (Zr – RE) alloy eutectic and the efficient grain refining effect of Zr.[2] The use of Mg has been largely limited by costs and limited technical capabilities versus alternative materials. There are few alloy elements that produce the desired properties.[2] The most common alloy element is Al, and secondarily Zn. A disadvantage of the as-cast Mg-Al alloys is the brittle Mg-Al $Mg_{17}Al_{12}$ β phase[2] sometimes called Mg_4Al_3, which forms directly without the formation of intermediate zones or precipitate in coarse laths on basal planes and in networks along grain boundaries where the hardening is needed; behavior which provides poor response to age hardening.[3] Furthermore, the β does not prevent grain boundary sliding mechanisms of elevated temperature creep deformation. The high melt temperature of the β phase at 437 °C in the Mg high-Al alloys causes hot shortness during extrusion at high rates.[2] Addition of Zn to the Mg-Al provides some hardening, but to prevent hot cracking of castings, the Zn amount which may be added is limited and the amount is inverse to the Al content.[3] Solution treatment may be used to improve properties; therefore, the Mg-Al and Mg-Al-Zn alloys are most often used as cast, or in the annealed, solid-solution treated condition, and inoculants are helpful to refine the as-cast structure. For the tough, ductile AM alloys increasing amounts of Al increases strength, but reduces ductility, an optimal Al amount is 6%. Aging of supersaturated AM50 and AM60 up to 2,000 h at 100 °C provides a 6% and 17% increase in ultimate and yield strength; however, with loss in ductility measured in 40% less elongation to fracture.[2]

2.3 Nomenclature of Alloys

No international designation code exists for Mg alloys. There has been a trend of using the method used by ASTM. Table A-1, Appendix A, presents the code letters for the principal alloy elements. In the ASTM method the first two letters (e.g., A = aluminum, Z = zinc), indicate the principal alloying elements, with the element of greater constituent quantity first or alphabetically if in equal quantity. The letters in group are then respectively followed by numbers, which designate the nominal composition rounded to the nearest whole number (e.g., AZ91 identifies Mg-9Al-1Zn). The next letter in group, suffix, designates the alloy generation or purity level (e.g., “A” generation 1, “B” generation 2), with “D” and “E” designation alloys of

high purity which attain high levels of resistance to general corrosion. The heat-treated or work-hardened tempers are designated as described for Al alloys.[3,6]

2.4 The Mg-Zn-Zr Wrought Magnesium ZW3 and ZK60A Alloys

The Mg-Zn-Zr alloys have advantage over Mg-Al and Mg-Al-Zn alloys in having potent solution and age-hardening, grain refinement, and freedom from the $Mg_{17}Al_{12}$ β equilibrium phase. The Mg-Zn-Zr alloys develop a fine grain, more homogeneous and tough structure adaptable to forging, extrusion, and heat treatment processes.[2,3] The mechanical properties of ZK60-T6 and ZK30-T6 extrusions have been reported as near isotropic in tension with good levels of ductility.[2] The Mg-Zn-Zr alloys are composed of constituents that are readily available and low-cost, with low levels of toxicity that effect biocompatibility and low risks to the environment. The processes of mining and metal refining are relatively simple and low cost. The wrought alloy provides mechanical properties of high material-class strength, ductility, and toughness with low sensitivity to notch-defect localized stress.[1–3] ZK60A is specified to have good resistance to stress corrosion,[2] but somewhat less resistance to corrosion than other Mg extrusion alloys, at 0.5–1.0 mg/cm^2/day mass loss in 3% salt solution.[4] The high strength ZK60 (Mg-6Zn-0.5Zr) alloy (ME) develops high room temperature strength as commercial off-the-shelf available wrought Mg alloys.[2,3] The Zr as a solute with the ZK sand-cast, or wrought material, promotes a refined grain structure that is beneficial to good formability, toughness, and fatigue resistance. The disadvantage of fine grain structure is low resistance to the grain boundary sliding mechanisms of creep deformation. The high levels of Zn in Mg (e.g., with ZK60A) lead to a wide solidification range of temperature, which lowers capability for fusion weld fabrication. The casting of Mg-Zr alloys requires special practices and the production method is batch practice.[2] Applications of ZK60A are specified for extruded rod, bar, tubing, shapes and forged shapes (e.g., aircraft wheels).[1,4] The ZK60A alloy may be electrical resistance welded.[1,4] The high yield and tensile strength ZW3 (ZK30, Mg-3Zn-0.6Zr) alloy has high compressive strength and further advantages of fusion weld capability under good conditions.[1] The ZW3-similar ZK21A Mg-2.0-2.6Zn-0.45Zr[20] is specified for inert gas shielded arc electric resistance weld methods, with arc welding filler metals AZ61A or AZ92A rod. The ZW3 alloy has capability for wrought work to multiple shapes (i.e., under British BSI 2L 505[7] there are standards for bars and extruded sections, sheet/strip under L504, and forgings/stock under L514). The multiple standards of wrought shape suggest capability for production of wrought shapes of plate and sheet. For consideration as a protection material, the ZK60A and ZW3 properties of high strength and toughness may be applicable to ballistic, or vehicle and crash

protection structures.[2] High strength is beneficial to improved levels of ballistic protection. Fine grain size is an important microstructure characteristic that enables the Hall-Petch strengthening mechanism[2,9] and unique combined improvement of yield strength, ductility, toughness, and resistance to stress corrosion crack propagation. Properties of combined strength and crack toughening are important material properties for protection material, which may enhance deformation and failure modes of plastic flow and resist deleterious localized deformation and brittle crack or cleavage-like fracture.

3. Experimental Materials and Test Procedures

3.1 Magnesium Alloys ZK60A-T5 and ZW3 Extrusion Materials

3.1.1 Melt-lots, Experimental Tests, Equivalent Thickness of Reference Comparison Materials

The source of the ZW3 and ZK60A-T5 Mg extrusion materials is Magnesium Elektron Ltd.* Table 1 identifies the experimental mechanical and V50 ballistic tests performed on specific melt-lots of the ZW3 and ZK60A-T5 profile extrusions and the nominal thicknesses. The mechanical property specifications for extrusions are often specified by specific area or thickness; Table 1 identifies the cross-section areas of the experimental extrusions. Table 2 presents representative thicknesses for specific values of weight/unit area, the areal density AD for the ZW3 and ZK60A-T5 experimental materials, and Al reference materials used in comparisons of the experimental ballistic protection performance. The range of ADs for the experimental profiles ranges from approximately 45 to 94 kg/m^2, approximately the weights of one-quarter to half-inch rolled homogeneous armor (RHA) steel. With the thicknesses scale of 12.7-mm thick RHA steel as a standard and 1× ratio, the Al thicknesses scale out in ratios of 2.8× to 3.0× thickness, Mg scales out to 4.3× to 4.4×, and the lightweight Mg-Li scales out to 5.4× thickness of RHA.

*Contract award W911QX-14-P-0481, 23 Sep-2014, Magnesium Elektron, now Luxfer MEL Technologies following merger with MEL Chemicals in 2018.

Table 1 Experimental ZW3, ZK60A-T5, thickness, melt number, experimental test outline

Alloy	Thick. (mm)	Melt	V50 Ballistic	Charpy	Hardness	Tension
ZW3	25.25	90087905 HQ12	X	X	X	X
ZW3	25.24	90088493 HS-1	X	-	-	-
ZW3	38.10	90087905 HQ10	X	X	X	X
ZW3	51.07	90087905 HQ-7	X	X	X	X
ZK60A-T5	25.36	90080423 HS-2	X	X	X	X
ZK60A-T5	38.09	90089288 HQ-8	X	X	X	X
ZK60A-T5	51.03	90089288 HQ-6	X	X	X	X

Notes: Thickness Area
Experimental profile-die cross-section areas: 25.4-mm, 1.0 inch = 9.79 inches sq. = 6,313 mm^2;
38.1-mm, 1.5 inch = 14.52 inches sq. = 9,366 mm^2;
50.8-mm, 2.0 inch = 19.14 inches sq. = 12,349 mm^2

Table 2 Equivalent thickness (mm) of magnesium, aluminum, and steel plate

	Magnesium (mm)					Aluminum (mm)			Steel (mm)
	Mg6Al	AZ31	ZW3	ZK60A	WE43	5083	7017	7020	RHA
Density (g/cm^2)	1.44	1.77	1.80	1.83	1.84	2.66	2.76	2.78	7.84
AD (kg/m^2)	Equivalent thickness (mm)								
24.90	17.27	14.07	13.83	13.61	13.53	9.37	9.02	8.96	3.17
49.80	34.54	28.14	27.67	27.21	27.07	18.74	18.04	17.91	6.35
99.60	69.07	56.27	55.33	54.43	54.13	37.47	36.09	35.83	12.70
199.2	138.14	112.54	110.67	108.85	108.26	74.94	72.17	71.65	25.40

Note: Densities of Al reference materials[21]

3.1.2 Nominal Composition and Mechanical Properties in Tension, Mg Wrought Alloys

Table 3 presents nominal compositions and mechanical properties in tension of wrought Mg alloys: 1) Mg-Zn-Zr ZW3, ZK60 alloys; 2) the RE-Y-Zr WE43 alloys; and 3) Mg-Al-Zn AZ wrought alloys. The direction of the material samples tested is longitudinal (L), the rolling direction (RD) for sheet or plate, or the direction of maximum flow of extrusions. The long traverse LT direction, sometimes called T direction, is parallel to the width of plate or sheet, or the diameter for solid extrusions. Technical reports on AZ31B-H24[12,22] and WE43-T5[13] materials present mechanical properties and ballistic performance. The WE43-T5 sheet[13] and to a much lesser amount the AZ31B sheet in the hard rolled condition[6] demonstrate directional dependent mechanical properties of lower yield strength and ductility in

the L orientation. The low limit of directional elongation in the WE43-T5 suggests that rolled WE43-T5 plate or sheet has low levels of toughness and resistance to shock and is susceptible to crack failure. The AZ31B rolled sheet in annealed condition appears near isotropic.[6] However, it has also been experimentally demonstrated in Mg extruded alloys there is anisotropy with lower yield strength in the T direction,[2,19] and higher strength in the L extrusion direction. Anisotropy in Mg alloys is not simple; it is dependent on the state of stress and crystallographic orientation, deformation temperature and history, mechanisms of texture and texture weakening with strain, deformation mechanism of twinning, solid solution hardening, grain size refinement, phase constituents, microstructure, and precipitation hardening.[19]

Table 3 Nominal compositions and tensile properties of wrought Mg alloys

ASTM standard	Nominal composition (%) Al	(%) Zn	(%) Mn	(%) Zr	Condition (shape)	Tensile properties 0.2% Y.S. (MPa)	T.S (MPa)	El. (%)	Character
AZ31-H24	3	1	0.3	-	Plate, 76.5 mm	169	262	9.5	MS, weldable, formable
AZ31B					Sheet	220	290	15	Hard rolled, parallel to RD (L)
AZ31B					Sheet	235	295	19	Hard rolled, perpendicular to RD (LT)
AZ61-F	6.5	1	0.3	-	Extrusions	180	260	7	HS, weldable
AZ80-T5	8.5	0.5	0.2	-	Extrusions	205	310	4	
	-	**RE**	**Y**	**Zr**					
WE43-T6	-	3	4	0.5	Extrusions	160	260	6	HT creep resistant
WE43-T5	-	3.5	4.0	0.5	Sheet	287	351	4.2	HT creep resistant, L orientation
	-					225	343	8.6	HT creep resistant, LT orientation
	Al	**Zn**	**Mn**	**Zr**					
ZW3	-	3	-	0.6	Extrusions	225	305	8	HS, formable
ZW3	-	3	-	0.6	EFS	205	290	8	Extruded forging stock
ZK60-T5	-	6	-	0.6	Extrusions	250	310	3	HS, formable, 1300 to 3200 mm^2
						235	310	5	HS, formable, 3200 to 16100 mm^2
						215	295	5	HS, formable 16100 to 25800 mm^2

Notes: medium strength (MS); high strength (HS); high temperature (HT); extruded forging stock (EFS);
rare earth element (RE); cerium (Ce); neodynium (Nd); yttrium (Yt); lanthanum (La); praseodymium (Pr).
Properties, Typical:
AZ61-F extrusions[3] Table 5.4;
AZ80-T6 forgings,[3] Table 5.4;
WE43-T6 extrusions[3] Table 5.4;
Properties, Test Performance:
AZ31B-H24: 76.48-mm H24 plate ARL-TR-4077 (2007),[22] sheet[6]
WE43-T5: ARL-RP-236, 4 mm sheet,[13];
Properties, Specification or minimum values:
ZK60-T5: ASTM B 107-13[1,5];
Magnesium Elektron: Datasheet 441 Elektron Wrought Alloys;[1]
ZW3: (Mg-3.0Zn-0.6Zr) British Standard: Aerospace Series Specification 2L 505: March 1973;[7]
Magnesium Elektron datasheet 441 for Extruded Forging Stock (EFS) 10-100 mm minor dimension.

The alloys of Table 3 are heat treatable for strengthening (e.g., with –F as fabricated, –T5 direct age, artificial age, or –T6 solution treat, quench, followed by artificial age). The AZ80, ZK60, WE43, and ZW3 are high-strength alloys; the AZ31 and AZ61 are medium-strength weldable alloys.[1–3] The WE43, ZK60A, and ZW3 contain Zr, which with specific treatment, is highly effective for grain refining and microstructure modification.[2,3] The Mg alloys cast with Zr as a grain refiner are less sensitive of the cooling rate to affect the microstructure. The alloy of maximum capability for extrusion speed is the AZ31 with 20 m/min capability; the AZ80 and ZK60A can have a lower extrusion speed of around 2 m/min.[2]

3.1.3 Standard Chemical and Mechanical Specifications of Mg ZW3 and ZK60A

Table 4 presents the standard specification requirements[5,7] of chemical composition and mechanical properties in tension of the experimental ZW3 and ZK60A-T5 Mg, along with the respective cross-section areas of the 25.4, 38.1, and 50.8-mm thick profiles. The area of the profiles all fall within 3,200–16,100 mm^2 area range for which Magnesium Elektron specifies the ZK60A-T5 properties of Table 4. The standard specification values for strength and ductility of ZW3 and ZK60A-T5 in the ranges approach near identical levels despite greater differences in chemical composition. The British Standard 2L 505 allows for significantly greater Zr content, and standardizes a more rigorous but not high-purity level, unlike ASTM B 107. A minimum level of 0.45 Zr in ASTM B107[5] appears low to obtain the full advantages of Zr for Mg-Zr alloy.[2,4]

Table 4 Standard-specifications, composition, Magnesium Elektron ZW3, ZK60A-T5 extrusions

Standard	Alloy	Zn (%)	Zr (%)	Mn (%)	Cu (%)	Al (%)	Si (%)	Fe (%)	Ni (%)	0.2% Y.S. (MPa)	T.S. (MPa)	El. (%)
BSI 2L 514	ZW3	2.5-4.0	0.40-0.80	0.15	0.03	0.02	0.01	0.01	0.005	205	290	8
BSI 2L 505	ZW3	2.5-4.0	0.40-0.80	0.15	0.03	0.02	0.01	0.01	0.005	225	305	8
ASTM B107	ZK60A-T5	4.8-6.2	0.45	-	-	-	-	-	-	235	310	5

Notes:
1. BSI 2L 505 March 1973: bars and extruded sections. Other standards: L504 sheet/strip; L514 forgings/stock;
2. BSI 2L 505 composition single values shown as maximum amount;
3. Magnesium Elektron Datasheet DS 441 refers to ASTM B107, single values shown as minimum, for areas of 3200 to 16100 mm^2, total other as impurities 0.30 maximum.
4. Composition values all weight percent; minimum values of strengths and elongation.

3.1.4 Certified Chemical Composition, Thickness, and Melt-Lots of the Mg ZW3 and ZK60A

Table 5 presents the certified chemical compositions of the experimental materials. The ZK60A-T5 materials have melt lots with 5.3 or 5.8 weight percent (%) Zn, well within the standard specification of 4.8 to 6.2%, and mid-range 5.5% Zn. The Zr levels range from 0.57 to 0.65%, which is greater than the ASTM B 107 0.45% minimum[4,5]; and, as demonstrated for sand casting of binary Mg-Zr alloys, Zr is a highly beneficial alloy element for grain refinement, strength, and elongation within the range of 0.45% through 0.65% up to around 0.80%.[2] It has been demonstrated that the tensile strength of the binary Mg-Zr alloys reaches peak level and remains constant for 0.55% or greater Zr. In the Mg-Zn-Zr sand casting alloys (e.g., ZK61A) the specification calls for 0.60 – 1.0 % Zr. The Zr in Mg alloys cast develops a fine hexagonal grain structure that promotes good flow behavior in sand or permanent mold castings. High levels of alloy purity benefit resistance to corrosion. The ZW3 alloy melt lots have Zn content of 2.9% and high levels of purity with Mn, Al, Cu, Ni, Fe, and Si totals under 0.029%, and Fe 0.003%. Fe contents above 0.002% increase corrosion rates.[2] Al, Mn, Si, Fe, Ni, Sn, Co, Sb, and H react with Zr to form detrimental intermetallic phases and microstructure; (e.g., Al_3Zr), which interferes with Zr solubility and the hardening and grain refinement, and optimal toughness; therefore Al and Mn are not deliberately alloyed with the MgZr alloys. The total Mn + Al is a low content of 0.015%. The mold-fill casting capability of Zr modified Mg alloys containing elements of Zn, RE, Ag, and Y is good due to the grain refining effect of Zr and a high volume fraction of eutectic phase, both which enhance fluidity.[2]

Table 5 Magnesium Elektron certified chemical composition, experimental profile extrusions

Alloy	Melt Lot (No.)	Thickness (mm)	Composition[a] (Weight %)							
			Zn	Zr	Mn	Al	Cu	Ni	Fe	Si
ZW3	90088493	25.4, 50.8	2.9	0.57	0.01	< 0.005	< 0.005	< 0.0005	0.003	<0.005
	90087905	25.4, 38.1, 50.4	2.9	0.65	0.01	< 0.005	< 0.005	< 0.0005	0.003	<0.005
ZK60A-T5	90080423	25.4	5.3	0.65	-	-	-	-	-	-
	90089288	25.4, 38.1, 50.8	5.8	0.61	-	-	-	-	-	-

Notes: Specifications: ZW3 BS 2L 505: 1973; ZK60A-T5 ASTM B107 - 13;
ZK60A-T5 total others < 0.30;
Not V50 tested: 90089288, 25.4 mm;
Certified chemical compositions for material delivered under contract award W911QX-14-P-0481, 23 Sep-2014.
[a]ZK60A-T5 Certificates: 96532, ME100 x 16″, Melt Lots 90080423, 90089288, Nov. 28, 2014;
96580, ME101 x 16″, Melt Lot 90089288, Nov. 28, 2014;
96306, ME102 x 16″, Melt Lot 90089288, Nov. 28, 2014;
ZW3 Certificates: 96533, ME100 x 16″, Melt Lots 90087905, 90088493, Nov. 28, 2014;
96581, ME101 x 16″, Melt Lot 90087905, Nov. 28, 2014;
96307, ME102 x 16″, Melt Lots 90087905, 90088493, Nov. 28, 2014.

3.2 Mechanical Test Procedures and Criteria

3.2.1 Charpy Impact Energy, and Instrumented Force, Energy, Displacement, Unstable Crack

Charpy impact toughness energy tests were conducted on UN 10-mm square × 55-mm Charpy specimens, LS orientation, with a Tinius Olson Model 84 machine equipped with a 60-pound (27.216 kg) hammer at impact velocity of 18.0 ft/s (5.5 m/s). Impact energy readings were obtained by Tinius Olson instrumentation; and, separately, IT (instrumented tup) readings of time, force, energy, and displacement that were recorded during tests. The plot of Fig. 1 defines the IT force versus displacement by example of a ZK60A-T5 UN Charpy specimen. Estimates of impact energy from ITs are approximate in numerical quantities; however, they illustrate the characteristic material response of deformation and fracture through force (F), energy, displacement (s), and time (t). The ASTM E-23 pendulum test type for impact energy derived from hammer velocity and mass is more reliable for energy estimates. The total impact energy W_t, general yield force F_y, maximum force F_m, crack initiation force F_{iu}, crack arrest force F_a, displacement at maximum load s_m, displacement at crack initiation (crack initiation displacement) s_{iu}, displacement at crack arrest (crack arrest displacement) s_a, and total displacement s_t follow respective definitions of energy, force, or displacement response under the ISO 14556 standard.[8] ISO 14556 specifies a typical deviation of 5J from the dial energy to the IT total impact energy; $W_{t;}$ deviations greater may result from machine friction, calibration, and software. The ISO 14556 test method defines measurements of time t, at beginning of deformation of the test piece $t_{0,}$ and signal rise time t_r. For protection material where extreme loading events are often short duration and high-intensity, the time duration for which protection material may either sustain load by ductile displacement or catastrophically fail by initiation of unstable crack propagation are important properties. This report provides more extensive time measurements for the Charpy IT, which supplement t_0, t_r with t measurements like the ISO 14556 displacements (see Fig. 1).

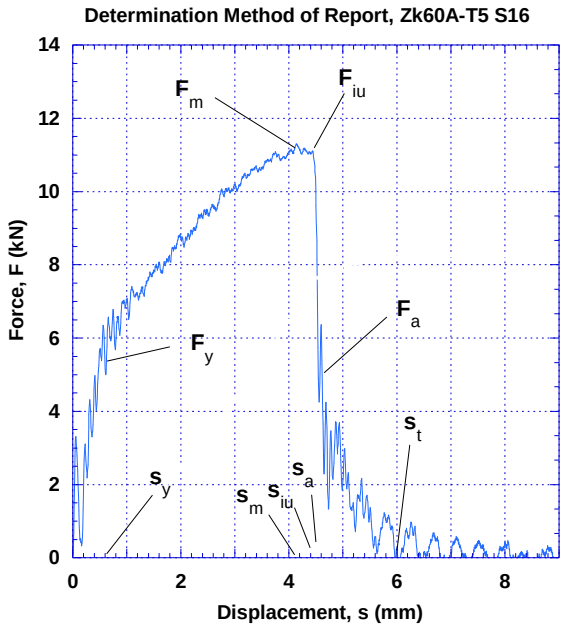

Legend, Instrumented Test (IT)

F_y = yield force;

F_m = maximum force;

F_{iu} = force to begin unstable crack propagation;

F_a = force at end of unstable crack propagation;

s_y = displacement at yield

s_m = displacement at maximum force;

s_{iu} = displacement, start unstable crack propagation;

s_a = displacement, end unstable crack propagation;

s_t = displacement, total

t_y = time at yield

t_m = time at maximum force;

t_{iu} = time, start unstable crack propagation;

t_a = time, end unstable crack propagation;

t_t = total time

Fig. 1 Plot, definitions, instrumented Charpy impact test, force (F), displacement (s), time (t)

3.2.2 Mechanical Tests in Tension and Analysis, Engineering Stress and Strain Properties

Tension tests were performed on an Instron 1123 mechanical test frame at a constant displacement rate of 0.0127-mm/s (0.03 inch/minute) until final fracture. Measurements of average uniaxial strain were obtained over a gage length of 1 inch by non-contact digital image correlation (DIC) measurement. Loads were obtained by output voltage of a calibrated 25-kN load cell. The test specimen geometry is subsize round, threaded-end tension specimens with 1-inch (25.4-mm) gage length and approximate diameter of 0.2533 inch (6.435 mm). The test specimens are the L-direction, the typical test direction specification of longitudinal direction[1,5,7,19] based on direction of maximum flow of the extrusion process. Digital data with load and strain were recorded with periods of either 0.10 or 0.20 s to final fracture. From the time increment load and strain data, and from measurements of final gage diameters, a Mathematica program plotted flow curves, and calculated values of Young's modulus and engineering stress and strain.

3.2.3 True Stress and True Strain in Tension, and Power Law Flow Curve Parameters

Engineering stress-strain curves do not give a true indication of deformation characteristics of metal because beyond load-drop of the maximum load region, in the tension test the material continues to strain harden and the stress increases

continuously up to final fracture. Therefore, true stress defines the actual stress when the load at any instant is divided by the instantaneous area of the minimum diameter. Up to maximum load, true strain is based upon actual instantaneous gage length of the sample, $\varepsilon = \ln(L/L_0)$, where L_0 is the original length and L the instantaneous length.[9] Beyond maximum load, the true strain in tension is measured by the actual area, $\varepsilon = \ln(A_0/A)$, where A_0 is the original area and A the instantaneous area. True uniform stress σ_u and true uniform strain ε_u describe the flow at maximum load. The true local necking strain ε_n describes true local strain from point of maximum load to final fracture ε_f. These strain levels describe global ε_u and local type ε_n ductility. The strain is uniform ε_u with respect to not fully localizing to point of stress and strain leading to fracture; in reality the strain is somewhat localized throughout deformation but the material adjusts load and deformation through work hardening or softening up to the point where the rate of strain hardening continually falls below level of flow stress. A Mathematica program calculated and fit true stress and strain parameters to maximum load at point of fracture, and fit the flow in the region of uniform plastic deformation to power law $\sigma = K\varepsilon^n$ hardening, where σ = true stress, ε = true strain, n = strain hardening exponent, K = strength coefficient.[9] The ε_i values designate the level of flow in true strain with which the power law begins to closely fit the flow curve that extends up to maximum load up to ε_u, σ_u. For power law flow the fully developed region of plastic flow expressed in true stress σ and true strain ε was equation fit in the linear region of log σ versus log ε. The power law describes true strain and flow stress σ and strain hardening, for which n = 0 is perfectly plastic, and n = 1 is perfectly elastic.

3.3 Microscopy Method

3.3.1 Optical Microscopy Procedure

Adequate optical microscopy (OM) results were obtained by sample sectioning with a water cooled soft-abrasive saw, mounting in epoxy, grinding with 320-, 400-, and 600-grit silicon carbide paper, polishing with nap-less cloth and oil lubricant with polycrystalline diamond first with 3-, then 1-micron diamond, with a final polish on soft short-nap cloth plus a commercial water-free colloidal aluminum oxide–silica suspension. Between polish steps the samples were cleaned with water and detergent, and rinsed and dried with alcohol. The final polished samples were etched with acetic-glycol (i.e., 1-mL HNO_3 + 20 mL acetic acid + 60 mL ethylene glycol + 19 mL H_20).

3.4 Ballistic Test Method, V50 Protection Criteria, Test Projectiles, and Targets

3.4.1 Targets

The ZW3 and ZK60A-T5 wrought material, the targets, were purchased as profile extrusions under contract W911QX-14-P-0481 23 September 2014. Custom dies were procured prior to extrusion of 25.4-, 38.1-, and 50.8-mm thick flat profiles 254 mm in width with full-thickness radius. The materials were delivered in sectioned lengths of 16 inches (406 mm) with the extrusion direction parallel to the length. Targets were used individually for the 0.30-cal. APM2 and 0.50-cal. FSP projectile tests. The targets for the 0.30-cal. APM2 tests were trimmed in length by 79 mm to provide sample material for microstructure and mechanical tests. The Mg alloy extrusion profiles[1] were purchased to British Standard Institution (BSI) 2L 505[7] for ZW3 alloy, and ASTM B 107-13 for ZK60A-T5.[5] The ZK60A-T5 artificial age temper may be obtained, for example, by extrusion then direct age 275 °F treatment for 48 h or by 300 °F for 24 h.[4] The F- condition is the as-fabricated condition. The T6 condition involves, for example, a 930 °F solution treatment for 2 h, hot water soft quench, and artificial age 300 °F for 24 h. BSI 2L 505 specifies condition to be "as extruded and straightened" with no heat treatment, which is the –F condition. The –F condition provides higher toughness and slightly lower strength than the T6 temper, in which grain growth may occur during solution treatment.[4] Table 5 shows the certified chemical compositions.

3.4.2 Ballistic Test Method and V50 Protection Criteria

The ballistic tests were conducted to obtain estimates of the V50 ballistic limit by the protection criteria BL (P).[10,11] The V50 ballistic protection test estimates penetration resistance using the mean value of protection calculated from fair impact velocities composed of an equal number of partial penetration (PP) and complete penetration (CP) impacts obtained over a limited range of impact velocities (e.g., 18.3 m/s [60 ft/s] for a 4-round V50 limit or 27.4 m/s [90 ft/s] for a 6-round limit). A CP occurs when the impact is fair, and the projectile or any fragment of the target or projectile perforates a witness plate (a 0.50-mm-thick Al-2024-T3 sheet) placed 152.4 mm (6 inches) behind the target. The V50 ballistic test provides a convenient proof or assessment of the penetration resistance and failure modes of actual protection materials that may not be entirely predicted by mathematical, physical, or material models. The tests targets of nominal 25.4-, 30.8-, and 51.8-mm thicknesses comprise an AD range of approximately 49.8- to 99.60 kg/m^2 (see Table 2 for the target material densities [g/cm^2], and equivalent

thicknesses). Chesapeake Testing*, Belcamp, Maryland, performed the 0.30-cal. APM2 V50 and 0.50-cal. FSP BL (P) tests.

3.4.3 V50 Test Projectiles

The projectiles[10] of the V50 tests are as follows:

1) Hard steel core 7.62-mm (0.30-cal.), armor-piercing APM2 projectiles weighing 165.7 grains (gr) or 10.74 g.

2) 12.7-mm (0.50-cal.) steel, FSPs of medium hardness, Rockwell C hardness HRC30, weight 207 gr (13.4 g).

4. Experimental Test Results and Discussion

4.1 Hardness Values of the Mg ZW3 and ZK60A-T5

Hardness value characterization is often practiced preliminary to ballistic testing either to help predict behavior or tensile strength, as part of a specification verification, or for insight in start test velocity for prototype test material. Table 6 presents the Rockwell E hardness (HRE) values, with results of approximately 69 HRE for ZW3 and 78 HRE for ZK60A-T5, obtained by through-thickness traverse of the experimental extrusion profiles. For soft steel or most soft non-ferrous alloys a value of 69 HRE, for ZW3, is equivalent to 61.5 HB Brinell hardness (500 kg, 10-mm ball). The experimental ZK60A-T5 approximate value of 77 HRE is equivalent to 65 HB.[6] The experimental HRE 78 is lower than typical ZK60A-F as-extruded shape hardness of 82–84 HRE,[4] or a direct aged ZK60A-T5 hardness of 88 HRE[6] and more near the hardness of ZK60A-T5 forgings which is described as 77 HRE or 65 HB.[6] The ZW3 material appears to have greater variance on average, and the variance appeared from a softer center to harder near-edge readings. There is no distinguishable hardness difference among the experimental melt lots of ZK60A-T5 despite a 90080423 melt lot certified level with 0.50 less Zn content. Hardness of Mg alloys is relatively low versus steel or aluminum; therefore design changes must be made in component design for stressed areas—for example, wall thickness typically greater with low wall thickness in low-stress areas; the seating areas require increase of area (e.g., 20% greater).

*Chesapeake Testing, Belcamp, MD, 21017, now National Technical Systems (NTS):
0.30-cal. APM2 test Jobs No. 2167-022: 1, 2, 3, 4, 5, 6, 7; 22-23 June 2015, Test report No. CT-RD-15-932;
0.50-cal FSP test Jobs No. CD01-2015-R05BLT-102: 121, 122, 125, 117, 132, 128; 31 August 2015.

Table 6 Experimental Rockwell E hardness, through thickness-traverse

Profile thickness (mm)	Tests no.	Alloy							
		ZW3				ZK60A-T5			
		Melt Lot	Average	SD	Spread	Melt Lot	Average	SD	Spread
25.4	5	90087905	69.0	1.1	1.7	90080423	77.8	0.7	0.5
38.1	7	90087905	69.6	1.0	2.0	90089288	77.9	0.7	1.1
50.8	9	90087905	68.6	1.3	3.0	90089288	77.7	0.7	1.4
All	21	All	69.0	1.2	4.1	All	77.6	0.7	2.6

Hardness test: Rockwell E hardness, 1/8-inch (3.175-mm) diameter steel ball, forces: 10-kgf minor-load, 100-kgf major load.
Extruded Profiles (MEL-100, ME-101, ME102), 254-mm widths.
Spread: maximum to minimum hardness decrease of profile, 2 test-average/position, 5-mm off edge, 5-mm off center.

4.2 Microstructure: Optical Microscopy of ZK60A-T5 and ZW3 Extrusions

The microstructures features resolved by OM at 1,040× and 2,080× are shown in Figs. 2 and 3 with the 25.4-mm flat profiles, and Figs. 4 and 5 with the 50.8-mm flat profile. The longitudinal direction of extrusion is parallel to the page width, and thickness direction is parallel to the page height. The profile thicknesses reveal similar complex microstructure features: a fine approximate average 10 μ grain size from recrystallization of hot wrought material; areas of broad localized shearing from the extrusion process; and on order of larger size of 50 μ to over 100 μ, what appears as a cast equiaxed grain solidification structure. Some microstructure effects of texture appear as shown in Figs. 2 and 4 with features of linear or segment-like neighboring recrystallized grains. From the linear segment-like microstructure of similar orientation grains, which suggests a texture effect,[19] it may be possible that in specific directions there is less effective Hall-Petch[2,9,19] yield strengthening effects of grain refinement and less than optimal resistance to crack propagation across the specific grain boundaries. The solidification structures with the 50–100 μ size features are more refined than the 100–200 μ grain size described from AlC_4 nuclei mechanisms.[2] Figures 2–4 reveal that the microstructures are consistent with a Zr refined cast microstructure with 50–100 μ size grains, further wrought with a recrystallized grain structure averaging 10 μ in size with either an –F or aged T5 temper.

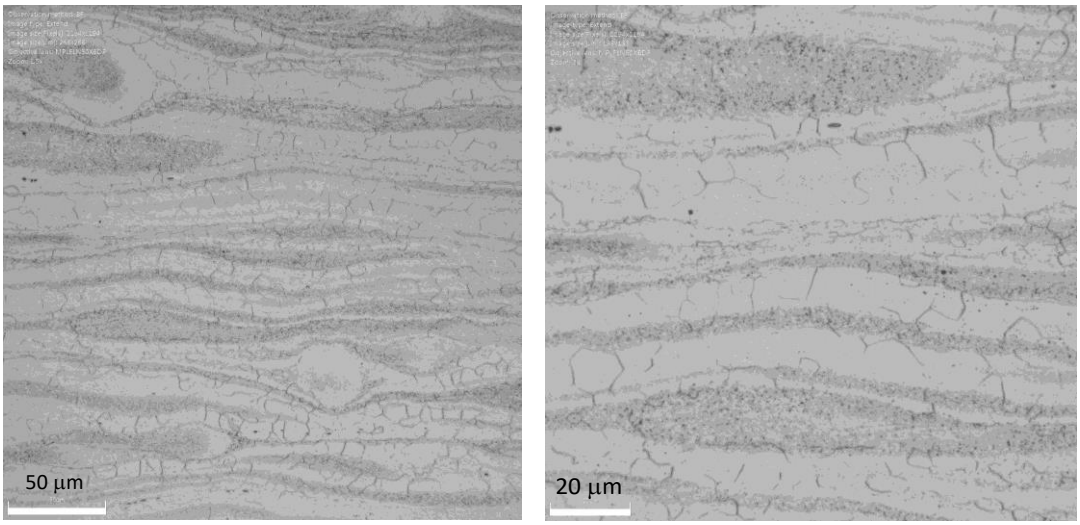

Fig. 2 Microstructure, ZW3, 25.4-mm profile, OM 1040× (left) and 2080× (right)

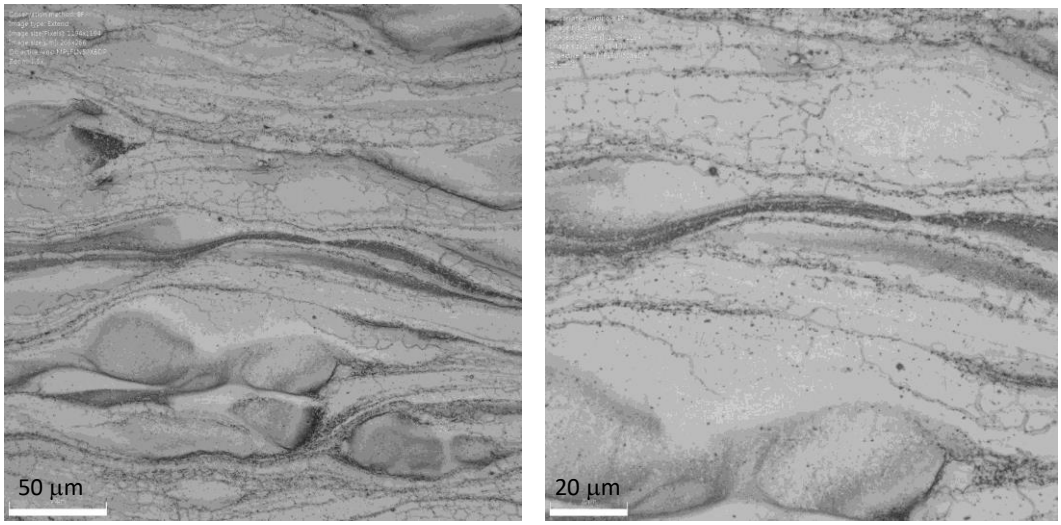

Fig. 3 Microstructure, ZK60A-T5, 25.4-mm profile, OM 1040× (left) and 2080× (right)

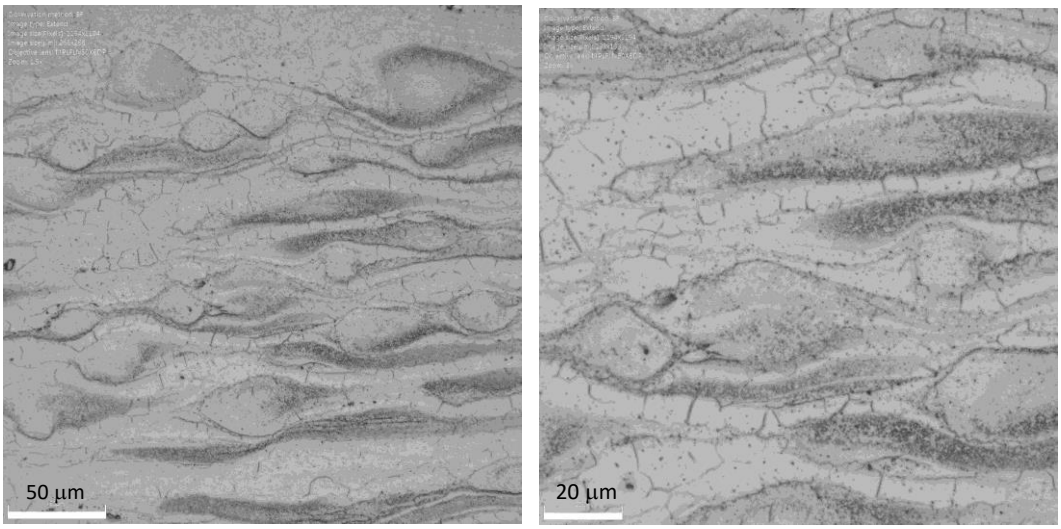

Fig. 4 Microstructure ZW3, 50.8-mm profile, OM 1040× (left) and 2080× (right)

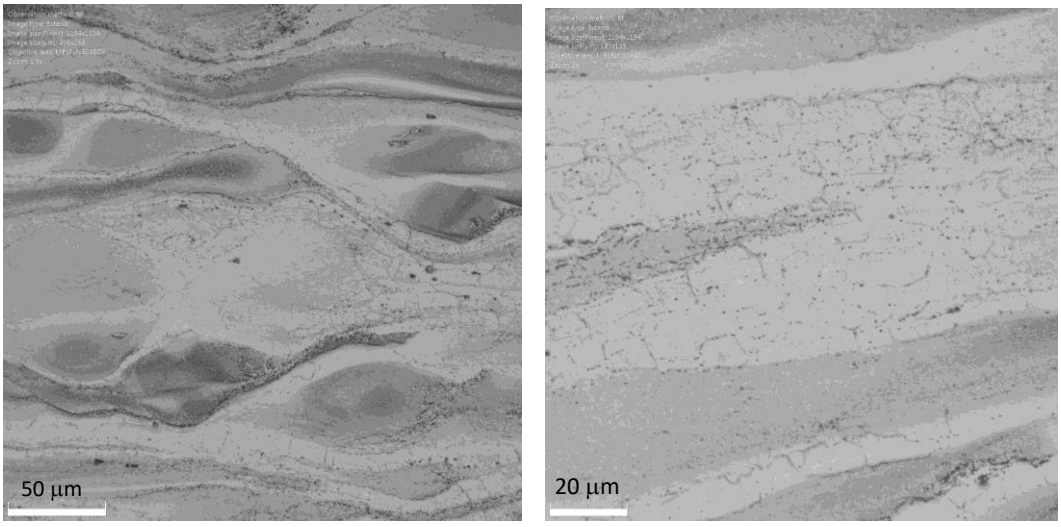

Fig. 5 Microstructure ZK60A-T5, 50.8-mm profile, OM 1040× (left) and 2080× (right)

4.3 Charpy Impact Test

4.3.1 Charpy Impact Energy Toughness

Table 7 presents the ASTM E-23 method impact energy toughness test results and standard deviations (SD) of UN wrought ZW3 and ZK60A-T5 Charpy specimens. The test orientation of the specimens is longitudinal – short transverse (LS) with the bar length parallel to the rolling direction and tup impact and crack propagation in direction of thickness, the S direction. However, one ZW3 specimen appeared to have been tested in the LT orientation with the result of a slightly greater amount of impact energy for that specific thickness. The 25.4-mm and 30.8-mm ZW3 and ZK60A wrought materials have relatively good toughness for Mg. On average the

toughness values decrease with increasing thickness of profile material. In comparison the impact energy of die cast UN Mg alloys have lower average toughness (e.g., 9 J for AZ91, 18 J each for AM60, AM50, and AM20, 16 J for AS41, and 12 J each for AS21 and AE42).[2] Therefore, the experimental ZW3 alloy has approximately 3× the toughness, and the ZK60A has 2.2×–2.7× the toughness as the AM alloy die cast UN specimens. The ZK60A-T5 impact tests results with 49.1 J and 46.4 J, respectively, of the experimental 25.4-mm and 38.1-mm profile source closely meet published performance property data[4] for UN rods and bar of –F temper listed at 35 ft-lbs (47 J) and –T5 temper at 34 ft-lbs (46 J); the 50.8-mm material toughness experimental data appears low in comparison to the published properties. The experimental ZW3 alloy provides high-impact energy in all thicknesses with more controlled loss of toughness with increasing thickness. The toughness results exceed the respective 31.9 J and 37.1 J impact energy for high-strength, high-purity, rapidly solidified ultra-fine grain LS orientation specimens of AMX602 and ZAXE1711.[23] The experimental results exceed UN Charpy impact energy of a compacted graphite cast iron (> 95 area % ferrite + 5 area % spheroidal graphite) with 32.1 J toughness, and the ASTM A 897 austempered ductile iron (ADI) tensile strength-yield strength-elongation 1400-1100-1 requirement of 35 J.[24] For specific toughness with an ADI density of 7.1 g/cm^3, the experimental Mg alloys exceed prior ADI impact energy results[25] and all ASTM A-897 ADI requirements (e.g., with the toughest 850-550-10 grade ADI, with specific toughness[24] by 1.7× – 6.5× for the experimental ZW3 and 1.2× – 5.5× for ZK60A-T5.

Table 7 Experimental Charpy impact energy toughness, UN bar specimens

Profile Thickness (mm)	Number of Specimens (No.)	Alloy							
		ZW3				ZK60A-T5			
		Energy		SD		Energy		SD	
		(ft-lbs)	(J)	(ft-lbs)	(J)	(ft-lbs)	(J)	(ft-lbs)	(J)
25.4	2	42.0	56.9	0.49	0.66	36.2	49.1	0.61	0.82
38.1	3	40.0	54.3	1.23	1.66	34.2	46.4	6.10	8.26
50.8	4	37.8	51.3	1.10	1.49	28.8	39.1	3.39	4.59
All	9	39.5	53.5	2.0	2.7	32.2	43.7	5.0	6.8

Notes: SD = Standard Deviation; LS specimen orientation.

4.3.2 Charpy Instrumented Impact Test: Force, Energy, Displacement, Time

Figure 6 presents the Charpy IT in LS orientation, experimental F, W, s characteristic results with plots of specimen 3 ZW3 and specimen 9 ZK60A-T5. Figure 7 presents plots of the characteristic F, W, and t for the identical specimens. Table B-1 in Appendix B reveals experimental quantitative result details of the

instrumented Charpy impact test average values and standard deviation statistic results with the number of tests n, per specific material; the sample profile, the forces F_y, F_m, F_{iu}, and F_a, the displacements s_m, s_{iu}, s_a, and s_t, and the total energy W_t. One ZW3 specimen (see Fig. B-1 in Appendix B) was tested in the LT orientation with distinctly different crack arrest s_a or F_a behaviors, which reveals capability for crack arrest or some resistance to crack growth. On average, the ZW3 clearly has greater plastic displacement characteristics with approximate average s_m 4.8 mm, s_{iu}, 5.8 mm, s_t, 6.4 mm versus ZK60A-T5 s_m 3.7 mm, s_{iu} 4.0 mm, and s_t 5.6 mm. The ZK60A consistently demonstrated crack arrest with values near F_a 3.2 kN and s_a 4.1 mm.

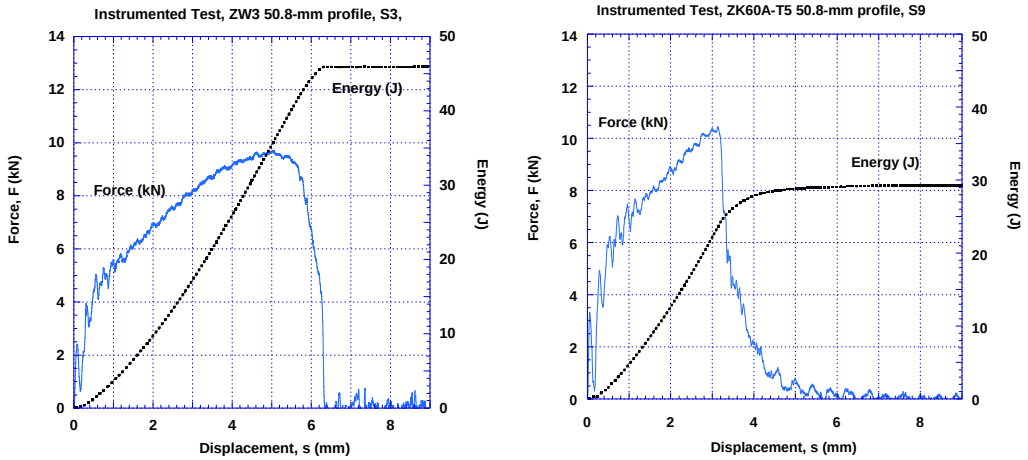

Fig. 6 Plots, experimental Charpy IT force, energy, displacement, ZW3 (left), ZK60A-T5 (right)

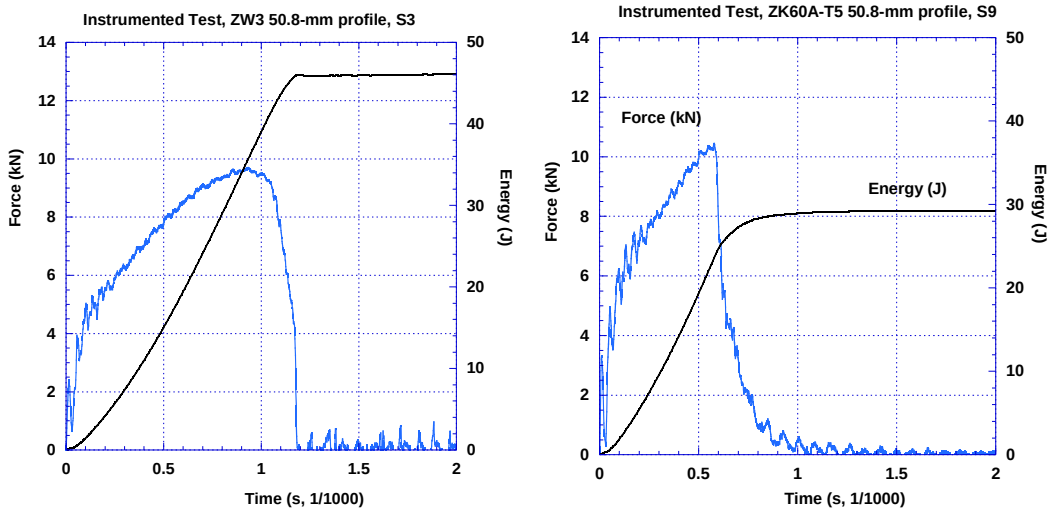

Fig. 7 Plots, experimental Charpy IT force, energy, time, ZW3 (left), ZK60A-T5 (right)

The average results of general yield strength with 5.1 kN for ZK60A-T5 are greater than the ZW3 4.3 kN force. Similarly, the ZK60A-T5 has moderately greater 11.2 kN maximum strength F_m levels than the 10.1 kN strength of ZW3. The ZW3 alloy in the LS orientation revealed excellent ductile fracture from high values of s_m and F_m with a substantial ductile fracture region of plastic displacement s_m to s_{iu}. The ZK60A revealed resistance to initiation of fracture followed by insignificant ductile fracture displacement between s_m and s_{iu}, but capability for crack arrest or resistance to crack growth in force with a region of s_a to s_t. The force – time plots reveal that ZK60A-T5 has 0.6 thousandths of a second t_m duration to maximum force similar to die cast DC AZ91[2] but at 10–11 kN, which is a significantly greater level of force versus 6.5 kN for DC AZ91. The 0.9 thousandths of a second t_m for ZW3 is similar to DC AM50[2] and greater than ZK60A. The specific time duration for ZW3 from start to unstable crack t_{iu} is 1.2 thousandths of a second (0.0012 s), which is 2× the crack initiation time t_{iu} of the 0.6 thousandths of a second of ZK60A. The ZW3 load duration outperforms in load and duration DC AZ91, AE42, AM60, AS21, and AM50 reference data of UN specimens that was tested with 3.9 m/s hammer speed.[2] The ZW3 outperforms the 6 kN load F_m of AM20;[2] and the ZW3 is outperformed only by AM20 in duration with a t_m of 0.00138 s (i.e., 1.38 thousands of a second).

4.3.3 Instrumented Test Characteristic Displacements, Crack Force Reduction

Table 8 presents the materials experimental deformation and fracture characteristics, in a manner less subject to variance of test and signal acquisition and analysis. On average, the proportion of force reduction by unstable crack growth (FRUC) is slightly greater for the high strength ZK60A-T5, but the proportions of force reduction by crack growth for both materials are near identical. Conversely, the proportion of ductile fracture surface (PDF), measured consistent with ISO 14556 Formula C.1[8] is slightly greater for ZW3. The differences are that ZW3 has greater proportions of displacement to maximum load and the initiation of fracture by unstable crack growth; and ZW3 has significant proportions and amounts of ductile fracture (DF) prior to crack initiation, but for the LS orientation tested, little resistance to crack growth or capability for crack arrest (DCA). Table B-2, Appendix B, presents the standard deviations of the test measurements.

Table 8 Charpy instrumented test, normalized plastic flow displacements and crack force-reduction

Target alloy	Profile source (mm)	Tests (n)	FRUC			PDF	Normalized ductile displacements			
			A	$(F_{iu} - F_a)$ (kN)	$/F_m$ (%)	$1 - (F_{iu} - F_a)/F_m$ (%)	s_m s_m/s_t (%)	s_{iu} s_{iu}/s_t (%)	DF $(s_{iu} - s_m)/s_t$ (%)	DCA $(s_t - s_{iu})/s_t$ (%)
ZW3	50.8	4	A	6.1	60.6	39.4	79.6	97.3	17.7	2.7
	38.1*	3	A	5.7	55.3	40.7	71.1	82.4	11.3	17.6
	25.4	2	A	7.3	71.8	28.2	75.0	96.8	21.8	3.2
	All	9	A	6.2	61.3	37.3	75.7	92.2	16.5	7.8
ZK60A-T5	50.8	4	A	7.2	62.6	32.2	64.1	66.2	2.1	33.8
	38.1	3	A	7.6	70.0	29.1	68.6	76.1	7.5	23.9
	25.4	2	A	8.6	74.9	25.1	69.8	74.0	4.2	26.0
	All	9	A	7.6	67.8	31.9	66.8	71.2	4.4	28.8

Notes: * One sample test with F_a = 6.798 kN, and s_a = 5.186 mm.
A = Average; SD = standard deviation;
F_y = general yield force; s_m = displacement at maximum force;
F_m = maximum force; s_{iu} = displacement, start of unstable crack propagation;
F_{iu} = force to begin unstable crack propagation; s_a = displacement at end of unstable crack propagation;
F_a = force at end of unstable crack propagation; s_t = total displacement;
FRUC = force reduction by unstable crack, absolute $(F_{iu} – F_a)$, normalized $(F_{iu} – F_a)/F_m$;
PDF = Proportion of ductile fracture surface (C.1 of ISO 14556: 2000)
s_m/s_t = ductile displacement to maximum load normalized to total displacement (NTTD);
s_{iu}/s_t = ductile displacement to initiation of fracture NTTD;
DF = ductile displacement by plastic fracture beyond F_m and prior to unstable crack extension NTTD, $(s_{iu} – s_m)/s_t$;
DCA = extent of ductile displacement by crack arrest resistance to crack propagation NTTD, $(s_t – s_{iu})/s_t$.

4.3.4 Charpy Test Scanning Electron Micrograph Fracture Features

Figures 8–13 reveal the fracture features of the 25.4-mm thick profile Charpy test specimens. The ZW3 specimen reveals extensive shear fracture (Figs. 8 and 10) for both impact and midsection regions. The ZK60A specimen reveals shear near impact regions only (see Figs. 8 and 13). The fracture features not obscured by shear (Figs. 9, 11–13) are on size-scale of grains similarly revealed by OM (Figs. 2–5); which suggest grain features of size, boundaries, and orientation affect deformation and fracture mechanisms, and that grain boundaries may serve as obstacles to strengthen material and limit fracture processes.[2,9]

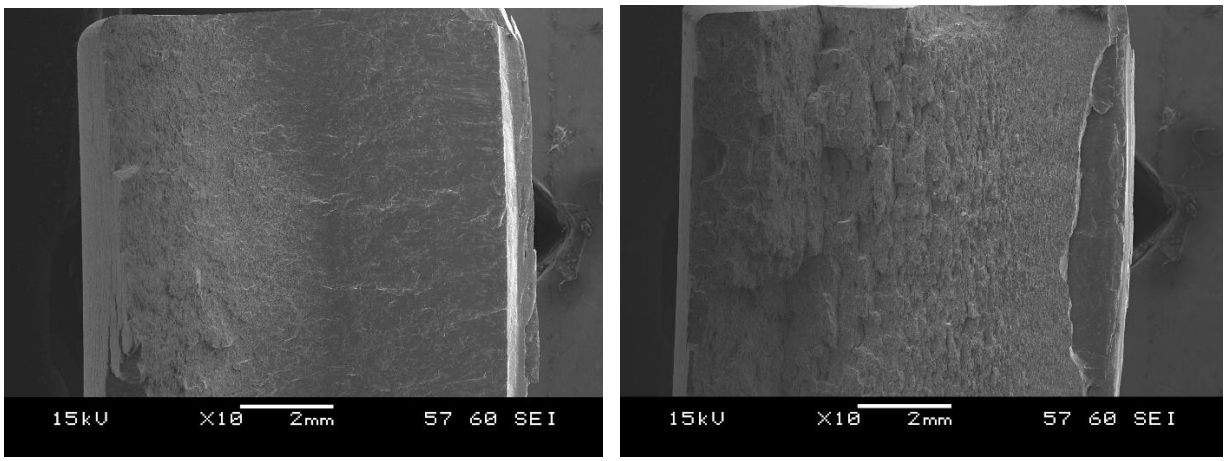

Fig. 8 Charpy test specimen SEM ×10, 25.4-mm profiles, ZW3 25.4 mm (left) and ZK60A-T5 25.4 mm (right)

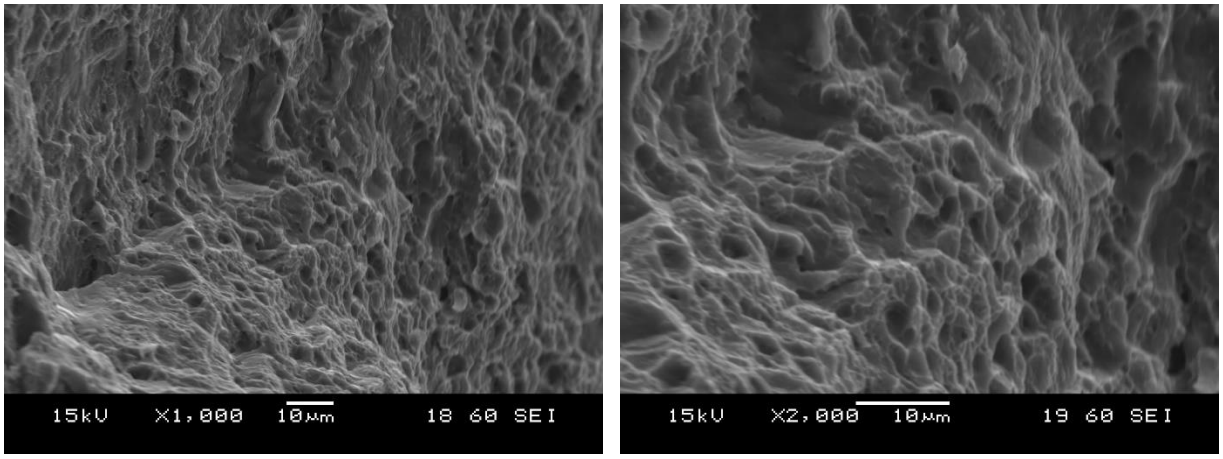

Fig. 9 Charpy test specimen ZW3 25.4-mm profile near final bend break, SEM 1000× (left) and 2000× (right)

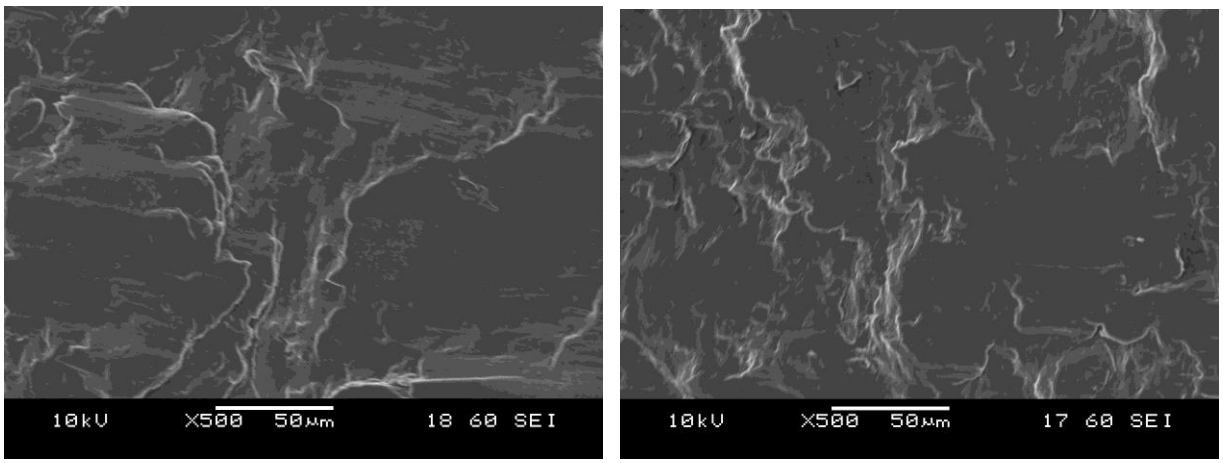

Fig. 10 Charpy test specimen ZW3 25.4-mm profile, SEM 500×, bend midsection (left) and tup impact (right)

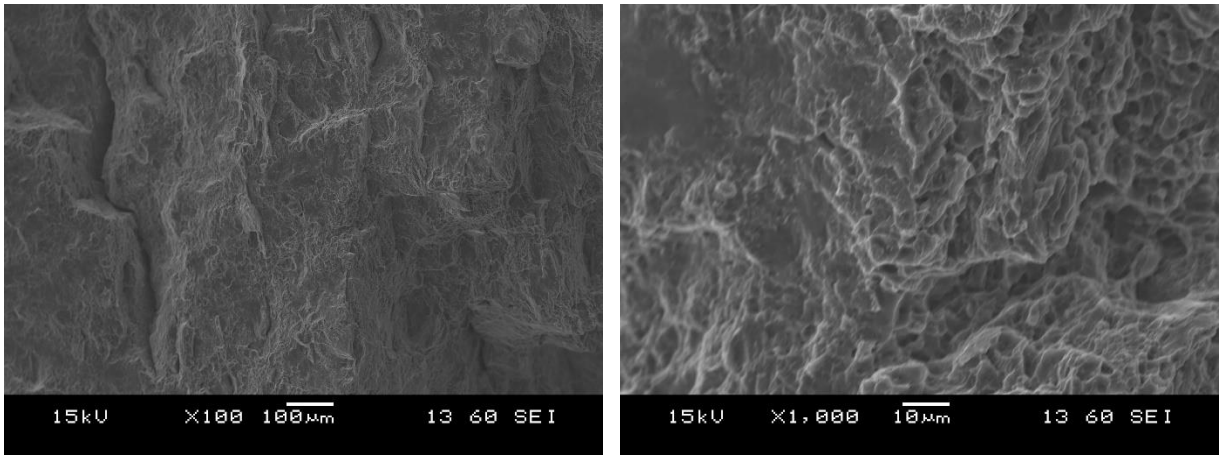

Fig. 11 Charpy test specimen ZK60A-T5 25.4 mm profile near final bend break, SEM 100× (left) and 1000× (right)

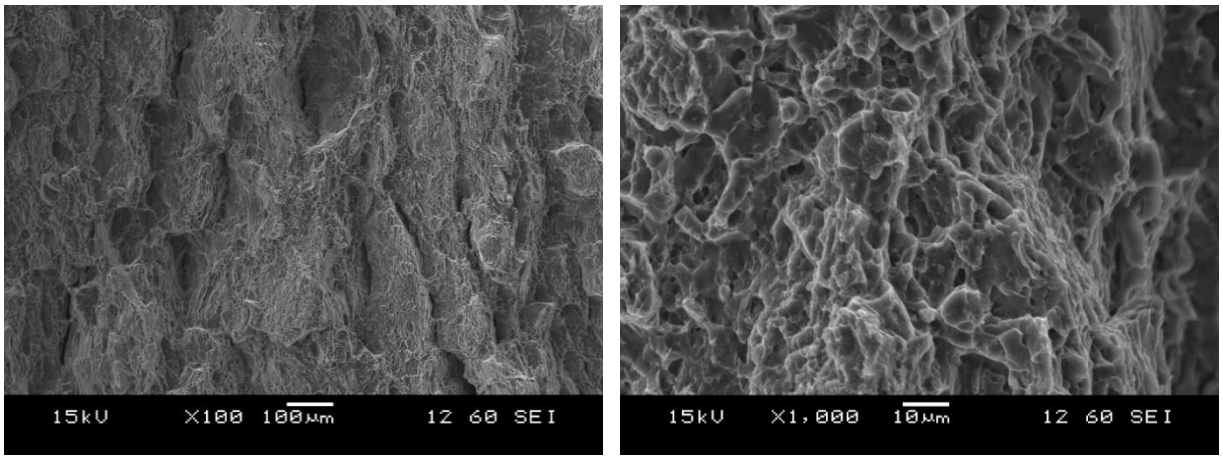

Fig. 12 Charpy test specimen ZK60A-T5 25.4-mm profile near midsection, SEM 100× (left) and 1000× (right)

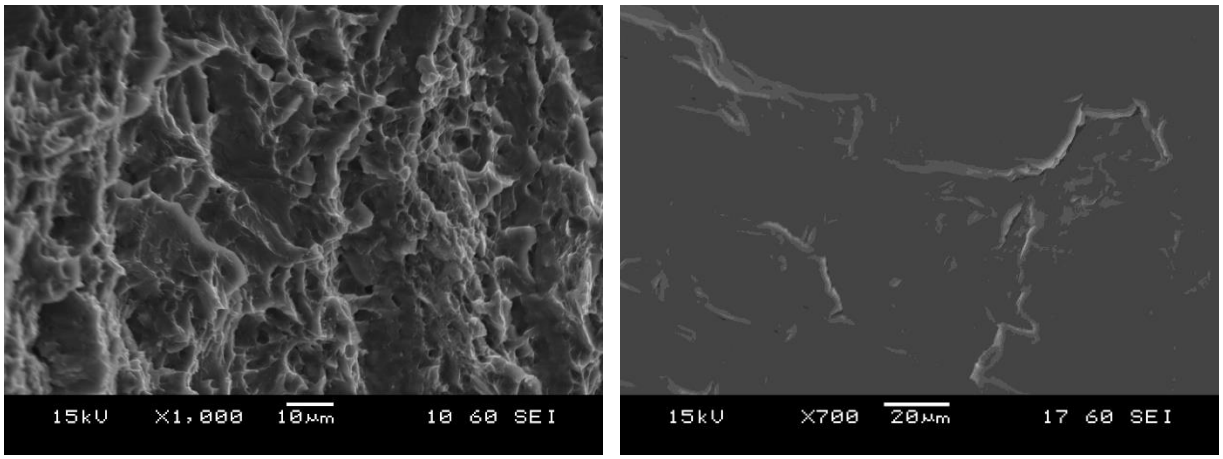

Fig. 13 Charpy test specimen ZK60A-T5 25.4-mm profile near impact, SEM 1000× (left) and 700× (right)

4.4 Mechanical Properties in Tension

4.4.1 Engineering Tensile Mechanical Properties, Yield and Tensile Strength Relations

Table 9 presents the experimental ZW3 and ZK60A-T5 engineering properties in tension based on instantaneous load and original diameter of test specimens. The test result and analysis values are Young's modulus, 0.2% offset yield strength (YS), tensile strength (TS), the ductility in percent elongation (El) reduction of area (RA), strain harden load increment TS-YS, and proportional strength YS/TS. The values are shown for test averages per profile thickness and alloy, and the average total results per alloy. The ZK60A-T5 results reveal higher strengths and lower ductility than the ZW3. Strain hardening measured by TS-YS is greatest with ZK60A-T5; however, both alloys have capabilities to strain harden, but the ratios of YS/TS appear low. The experimental test values of the ZK60A-T5 are close to and meet on average the minimum YS 36 ksi (250 MPa), and TS 45 ksi (310 MPa) requirements of ASTM B 107-13 for bars, rods, shapes, and wire, for profile areas of 3,200- to 16,100 mm^2. The ZK60A-T5 experimental elongation values, which average 14%, far exceed the ASTM B 107 requirement of 3–5% elongation. The RA levels are low, possibly somewhat influenced by the minimum initial gage diameter that was machined near end of gage length. Table B-3, Appendix B, presents the standard deviations of mechanical properties in tension.

Table 9 Experimental engineering stress and strain in tension, ZW3, ZK60A-T5 extrusions

Alloy	Profile	No. Specs.	YM (GPa)	YM (Msi)	YS (MPa)	YS (ksi)	TS (MPa)	TS (ksi)	El (%)	RA (%)	TS-YS (MPa	YS/TS
ZW3	25.4	2	44	6.4	225	33	285	41	19	25	60	0.79
	38.1	2	42	6.0	222	32	283	41	20	34	61	0.79
	50.8	3	43	6.2	211	31	275	40	20	31	64	0.77
	All	7	43	6.2	218	32	280	41	20	30	62	0.78
ZK60A	25.4	2	45	6.6	258	37	319	46	14	20	61	0.81
	38.1	2	46	6.7	246	36	315	46	14	22	69	0.78
	50.8	3	47	6.8	245	36	314	46	13	21	68	0.78
	All	7	46	6.7	249	36	316	46	14	21	67	0.79

Notes:
YM = Young's modulus
YS = 0.2 percent offset yield strength
TS = ultimate tensile strength at maximum load
El = elongation in percent (final length – initial length)/initial length
RA = reduction of area %

Specifically, 7 of 7 ZK60A-T5 specimens passed YS requirements for 235 MP, with 5 of 7 passing the requirement of 310 MPa TS. The typical properties of ZK60A-T5 are specified as 44 ksi YS (303 MPa), 53 ksi (365 MPa) TS, with 11%

elongation.[4] The two specimens of lower 5.3 % Zn content of ZK60A-T5 Melt-Lot 90090423 in 25-mm thickness profile shape passed the ASTM B 107 strength requirements and the strengths of the Melt-Lot 90090423 in 25-mm thickness were slightly greater than average; therefore, there was no deleterious effect of low Zn content on strength. In comparison to 3 mm and 1.5 mm thick thin sheet ZK60 conditioned to ultra-fine grain size by alternate biaxial reverse corrugation (ABRC),[26] the experimental ZK60A-T5 results of Table 9 demonstrate superior yield and tensile strength and approximately equal elongation ductility. Except for the 25.4-mm profile YS, the experimental test values of the ZW3 on average do not meet minimum YS 33 ksi (225 MPa) and TS 44 ksi (305 MPa) requirements of BS 2L505-1973 for bars and extruded sections, for minor sections over 10 and up to 100 mm. The ZW3 experimental elongation values, which average 20%, far exceed the requirement of 8% elongation; and the high values of ZW3 L-direction elongation ductility suggests ZW3 rolled plate may provide acceptable levels of T-direction ductility and toughness. No heat treatment is specified for the BS 2L505-1973; the material specification is as-extruded and straightened. The properties of ZW3 by average value meet the BS 2L505-1973 specification for under 10-mm minor thickness (i.e., 29 ksi YS [200 MPa], 41 ksi [280 MPa] TS, with 8% elongation). Specifically, 2 of 7 specimens passed the BS 2L505 YS requirements for 225 MP, with 0 of 7 passing 305 MPa TS; 7 of 7 passed 200 MPa YS, and 6 of 7 passed 280 MPa TS. For the BS L514 extruded forging stock EFS standard,[1] the ZW3 samples all meet the 205 MPa requirement for YS, but are slightly low in the 290 MPa requirement for TS. The failure to meet specification requirements may be due to minimal diameters that were machined near ends of gage lengths and the surface finish of the tension test specimens; and there may be effects of material quality (e.g., directional-dominant extrusion strain, which aligns deformation texture of recrystallized grains). Aligned textured or non-random oriented grains may be deleterious to the Hall-Petch effect of hardening and resistance to crack propagation.[19]

4.4.2 Engineering Plastic Flow and Fracture Behaviors

Figure 14 plots examples of experimental plastic flow curves with engineering stress versus engineering strain to fracture. These flow curves do not have well-defined yield strengths observed with high-strength grain-refined powder metallurgy alloys AMX602 or ZAXE1711.[23] The engineering flow curves demonstrate a significant amount of strain and exceptional strain hardening to maximum load, followed with an extended region of fracture ductility strain beyond maximum load.[2] Al alloy 2024-T351, T orientation, with higher strengths, demonstrates similar early plastic flow yield and work hardening behavior.[27] Other than the indefinite gradual yield strength region, the lower flow stress, and greater

fracture ductility, the ZW3 flow elongation approximates strain levels of Al alloy 6061-T651.[27] The ZK60A-T5 behavior resembles flow of Al 7075-T7351 or 7475-T7351[27] in the L direction at lower levels of strength.

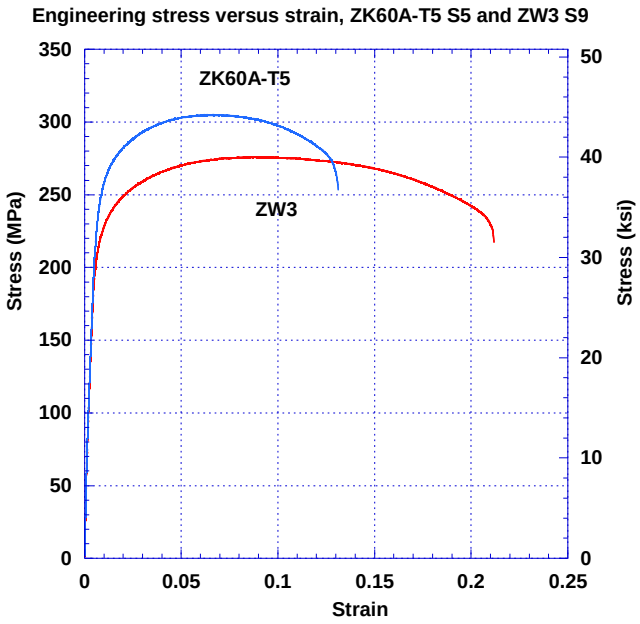

Fig. 14 Plots, plastic flow in tension, engineering stress vs. strain, experimental ZW3, ZK60A-T5

4.4.3 True-stress True-strain, and Strain Hardening Exponents and Strength Coefficients

Table 10 presents the true uniform stress σ_u and true uniform strain ε_u mechanical properties in tension up to maximum load, at the point of final fracture the true fracture stress σ_f and true fracture strain ε_f; the true necking strain ε_n beyond maximum load to final fracture ε_f, and the parameters for power law plastic flow. The ZW3 demonstrates greater true strain ε_f to fracture, and greater local fracture ductility with true necking strain ε_n. The ZK60A-T5 reveals greater true levels of strength, with advantage in true fracture stress σ_f. In comparison to grain-refined powder metallurgy AMX602 or ZAXE1711[23] alloys from the Spinning Water Atomization Process (SWAP), the true stress σ values are low, the true ε_u low, but ε_f, and most specifically the ε_n are greater. The SWAP materials demonstrate power law flow curves, to maximum load, with greater K and n. The power law flow fits and parameters were verified in range and accuracy of fit (see Fig. B-2 in Appendix B) by direct comparison to plastic flow to σ_u, ε_u. In comparison to plastic flow of Al alloys 7075-T7351 or 7475-T7351, ZW3 has lower strength and flow

values similar in e_u, e_n and the power law n.[27] Table B-4, Appendix B, presents the standard deviations of the true stress true strain and power law properties.

Table 10 Experimental test true stress and strain in tension, flow curves, ZW3, ZK60A-T5

Alloy	Profile	No. Specs.	True: stress σ, strain ε					Flow curve $\sigma = K\varepsilon^n$		
			σ_u (MPa)	ε_u	ε_n	σ_f (MPa)	ε_f	n	K (MPa)	ε_i
ZW3	25.4	2	311	0.09	0.20	312	0.29	0.11	412	0.020
	38.1	2	308	0.08	0.33	336	0.41	0.11	405	0.020
	50.8	3	300	0.09	0.29	305	0.37	0.12	401	0.020
	7-Tot.	Ave.	305	0.09	0.27	316	0.36	0.11	405	0.020
ZK60A	25.4	2	339	0.06	0.17	335	0.23	0.09	436	0.025
	38.1	2	337	0.07	0.18	345	0.25	0.10	440	0.025
	50.8	3	334	0.06	0.17	339	0.23	0.10	438	0.025
	7-Tot.	Ave.	336	0.06	0.17	339	0.24	0.09	438	0.025

Notes: σ_u = true uniform stress; ε_u = true uniform strain;
ε_n = true necking strain;
σ_f = true fracture stress; ε_f = true fracture strain;

4.4.4 Comparisons of Specific Modulus and Strengths to Engineering Materials

Specific modulus YM/ρ, the specific yield strength YS/ρ, and the specific tensile strength TS/ρ reveal weight efficiencies for a unit volume of material. The listed value of Young's modulus for Mg alloys is 6.5×10^6 psi or 45 GPa[2,6]; however, the elastic modulus of material is somewhat variable through material alloy design and processing, and material products are not perfect in homogeneity and isotropic properties. Table 11 presents some comparisons of specific modulus and specific strength for the experimental Mg ZW3 and ZK60A-T5 alloys. The Al comparison alloys and applications are 6022[28] and 6451 (automobile skin),[29] 6061 (vehicles and structures), 2024, 7475, 7075, 7475[27], 7055[30], and the 2195[30] and 2196[31] Al-Li (aerospace) materials. Except ZK60A-T5, the experimental ZW3 and reference Mg alloys[32] have an equal or lower specific elastic modulus than either aluminum, titanium,[33] or steel[34,35] materials. With the materials shown, the Al-Li aerospace alloys are most efficient in providing high specific modulus; and there has been a long history to the present in investment, development, and application to aircraft. Furthermore titanium provides the second best specific modulus; low alloy steels are third. The experimental ZW3 and ZK60A-T5 YS/ρ and TS/ρ values exceed the automotive skin alloys 6022, 6451 and structure alloy 6061 Als, and are lower than the WE43-T5 Mg, the aerospace Als, Ti-6Al-4V, and steel. Mg sheet is not readily cold formed but may be deep drawn with optimal warm temperature and strain rate.[2,3] The wrought work forming method of hydrostatic extrusion is a method for Mg fabrication that enhances extrusion-forming capability at lower temperatures

and important grain refinement, and that can prevent microcracking fracture.[2,3,36] The hydrostatic extrusion method at lower process temperature effects mechanisms of Hall-Petch grain-refinement strengthening[2,3,9] and toughening, and unlike solid solution or precipitate hardening mechanisms the Hall-Petch mechanism does not effect a great loss in ductility or toughness. In conventional fabrication practice, multiple-passes with temperature control and preliminary and final steps of forming may be used to refine grain size. Therefore, the hydrostatic extrusion, or multiple pass methods may provide a wrought forming process method for light metal and Mg alloys to achieve higher efficiencies in specific YS/ρ and TS/ρ.

Table 11 Specific-strength properties and comparisons, experimental ZW3, ZK60A-T5

Material	Alloy	Temper	Density (g/cm^3)	YM (GPa)	YS (MPa)	TS (MPa)	YM/ρ (GPa cm^3/g)	YS/ρ (MPa cm^3/g)	TS/ρ (MPa cm^3/g)
Mg	ZW3	-F	1.80	43	218	280	24	121	156
	ZK60A	-T5	1.83	46	249	316	26	136	176
	AZ31	-H24	1.77	45	186	269	25	105	149
	WE43	-T5	1.84	45	287	351	25	156	195
Al	6022	-T43	2.69	70	227	294	26	84	109
	6451	-T6	2.70	70	250	290	26	93	107
	6061	-T651	2.64	70	300	328	26	111	121
	7020, 20/46	-T651	2.78	70	360	408	25	129	147
	7020, 11/46	-T651	2.78	70	369	414	25	133	149
	7020, 03/46	-T651	2.78	70	381	425	25	137	153
	2024	-T351	2.79	72	407	519	26	146	187
	7475	-T7351	2.81	71	464	531	25	165	189
	7075	-T651	2.79	71	552	608	25	196	216
	7055	-T7751	2.87	71	602	632	25	210	221
	2195	-T8	2.71	76	592	627	28	218	231
	2196	T8511	2.63	77	490	538	29	186	205
Ti	Ti-6Al-4V	annealed	4.42	122	828	895	28	187	202
		RLC	4.42	112	905	970	25	205	219
		STA	4.42	122	1034	1100	28	234	249
Fe	RHA Steel	440	7.84	210	1175	1380	27	150	176
	HH Steel	500	7.84	210	1310	1655	27	167	211

Notes: see Friedrich and Mordike[2], p. 317;
Mg, Al, Ti properties given for the longitudinal (L) direction, steel properties are typical;
AZ31-H24 density, and strengths from ARL-TR-4327,[32] listed modulus[6];
WE43-H24 density properties and strengths from ARL-RP-236[13], listed modulus[6];
Al densities from AA 2018 Teal Sheets[21]; 7020-T651 strengths from ARL TR-7986[16];
Al 6061, 2024, 7475, 7075, 7055, 2195 modulus and tensile properties from ARL-TR 4596[27];
Al 2196 strengths from Gérard Uféras, Airware© 2196-T8511 Extrusions, brochure, Constellium, May 2007[31];
Ti-6Al-4V Annealed, modulus, Timetal datasheet TMC-0150, 2000[33]; Solution treated, aged STA, Timetal datasheet TMC-0150, 2000; Rolled low-cost (RLC); solution treated and aged (STA); Steel: Evraz, Armalloy 440T Armor Plate, datasheet and MIL-DTL-12560J 4a[34]; Evraz, Armalloy 500HH Armor Plate, datasheet and MIL-DTL-46100E[35]

4.5 V50 Ballistic Protection Experimental Tests

4.5.1 V50 Experimental Target Parameters, V50 Ballistic Test Results and Statistics

Table 12 presents V50 ballistic protection test results for a limited number of ballistic impacts for nominal-thickness targets of 25.4, 38.1, and 50.8 mm of the ZW3 and ZK60A-T5 experimental flat profile extrusions. The limited number of test impacts in each V50 appear to have affected statistics in the test spread and standard deviation (SD). In these tests, the number of V50 impacts that achieve the required test spread and lowest SD of impact velocity are the criteria for choice to select either a 4-round or 6-round V50 velocity. Despite limited amounts of V50 test data, the ZK60A-T5 and ZW3 SD levels for individual 0.50-cal FSP tests are equal or slightly larger than the moderate high deviations of 7039 aluminum (e.g., 11.3–16.5 m/s), and equal or less than high deviations for RHA or high hard steel HHS (e.g., 18.0 m/s).[10] The 0.30-cal. APM2 V50 tests performed with ZK60A-T5 have the lowest test spreads. The ZK60A-T5 and ZW3 SD levels for the 0.30-cal. APM2 are less than for RHA (e.g., 15.6 m/s), and less than 7039 Al (e.g., 12.2 m/s), with ZK60A-T5 having low SD levels near 5083 Al (e.g., 8.84 m/s).[10] Other than one test for each material, the 0.50-cal. FSP tests did not meet requirements for 18 m/s 4 round, or the 27 m/s or 46 m/s velocity spreads for 6-round V50 tests. The protection levels of the test plates did not achieve full muzzle velocity 0.30-cal. APM2 level protection of approximately 841 m/s.[11] The ZK60A-T5 appears to provide slightly better 0.30-cal. APM2 protection, and with some mixed results the ZW3 provides slightly better 0.50-cal. FSP protection.

Table 12 Experimental target parameters and the V50 ballistic test results and statistics

Projectile Type	Target				V50 Protection Limit								
	Impact Obliquity (°)	Alloy	Thick (mm)	AD (kg/m^2)	Target Impacts (No.)	V50 Shots (No.)	High Partial (m/s)	Low Complete (m/s)	Spread (m/s)	RMR (m/s)	Gap (m/s)	V50 (m/s)	SD (m/s)
0.50-cal. FSP	0	ZW3	25.20	45.37	7	4	549.6	557.2	18.9	-	7.6	556.8	9.8
	0	ZW3	37.86	68.15	7	4	817.5	840.9	37.8	-	23.5	828.8	18.2
	0	ZW3	50.95	91.71	7	2	1152	1207	54.3	-	54.3	1180	-
	0	ZK60A-T5	25.36	46.40	7	6	542.5	558.1	41.8	-	15.5	543.7	18.8
	0	ZK60A-T5	38.04	69.62	7	4	812.9	832.7	40.2	-	19.8	820.0	18.6
	0	ZK60A-T5	51.02	93.36	7	4	1216	1189	29.0	26.8	-	1205	14.2
0.30-cal. APM2	0	ZW3	25.25	45.47	6	6	492.6	477.9	33.2	14.6	-	479.8	13.2
	0	ZW3	25.24	45.43	7	4	454.8	472.1	21.9	-	17.4	463.4	11.4
	0	ZW3	38.10	68.58	7	4	589.5	596.2	18.3	-	6.7	591.8	8.0
	0	ZW3	51.07	91.92	9	6	688.8	705.6	23.5	-	16.8	696.3	11.5
	0	ZK60A-T5	25.36	46.40	8	4	473.7	480.1	18.3	-	6.4	474.0	8.6
	0	ZK60A-T5	38.09	69.71	10	4	605.9	604.1	16.4	1.8	-	603.7	6.4
	0	ZK60A-T5	51.03	93.39	7	4	712.0	720.2	12.8	-	8.2	717.3	6.9

Notes: (1) Test impacts numbers (No.) shown for within and beyond the range of velocities (the spread) of the V50:
RMR = range of mixed results, not shown: the results are completes (C) all at high range of V50 spread and/or above; partials (P) all at low V50 spread or below;
Id. = test data target identity;
(2) Gap = velocity difference of low C and high partial for a test with no RMR; SD = standard deviation of the V50 test;
(3) ZW3 of standard BS 2L 505 chemical composition; ZK60A-T5 of ASTM B107/B107M-13 chemical composition;
(4) Tests performed under the Protection Criteria.

4.5.2 V50 Ballistic Test Failure Modes

Ballistic V50 failure modes for the 0.30-cal. APM2 tests of Figs. 15–18 demonstrate toughness with ductile-hole growth near impact or exit points, and near-complete absence of any fragmentation, spall, plugging, or extensive cracking despite high-velocity impacts. The failure modes of the 0.50-cal. FSPs of Figs. 19 and 20 again demonstrate toughness with spall being closely limited to regions of previous and concurrent plastic flow, with the plastic flow a combination of ductile-hole growth and petal-like fracture. The localized spall demonstrates multiple delamination-like cracking near impact and exit points. The FSP spall and cracks extend less than 2 projectile diameters in radius from the impact points, around 1 projectile diameter in radius for ZW3, and greater than 1 projectile diameter for ZK60A-T5; therefore IT Charpy tests and ballistic V50 FSP tests appear consistent to demonstrate toughness. Extent of target material resistance to cracking may be better determined from impacts of large diameter projectiles.

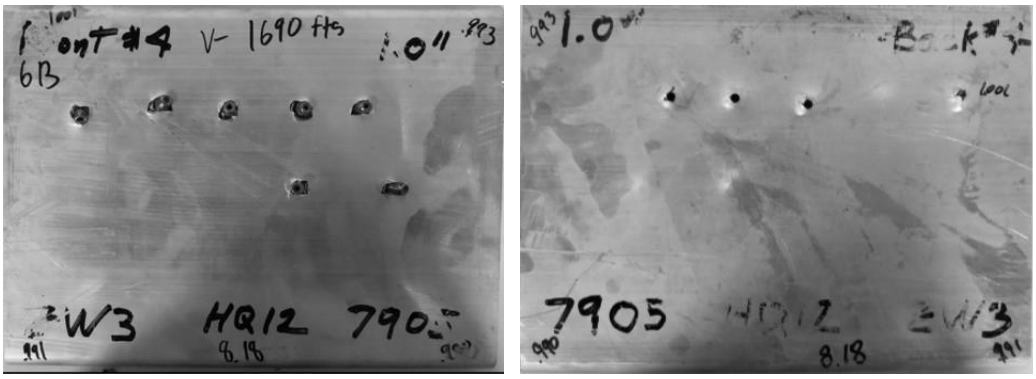

Fig. 15 ZW3 25-mm profile target vs. 0.30-cal. APM2, 0° obliquity, front (left) and back (right)

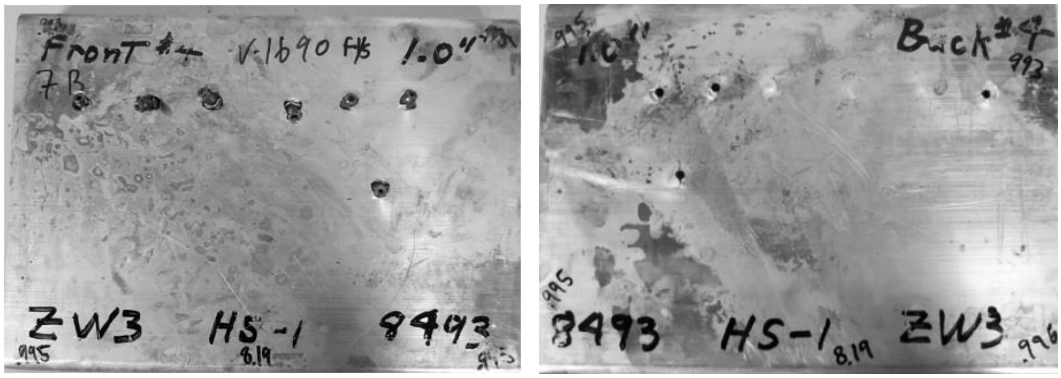

Fig. 16 ZK60A-T5 25-mm profile target vs. 0.30-cal. APM2, 0° obliquity, front (left) and back (right)

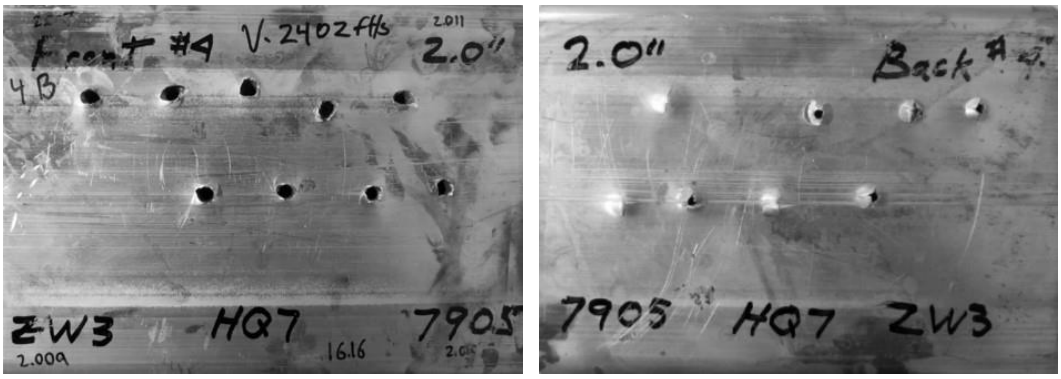

Fig. 17 ZW3 50.8-mm profile target vs. 0.30-cal. APM2, 0° obliquity, front (left) and back (right)

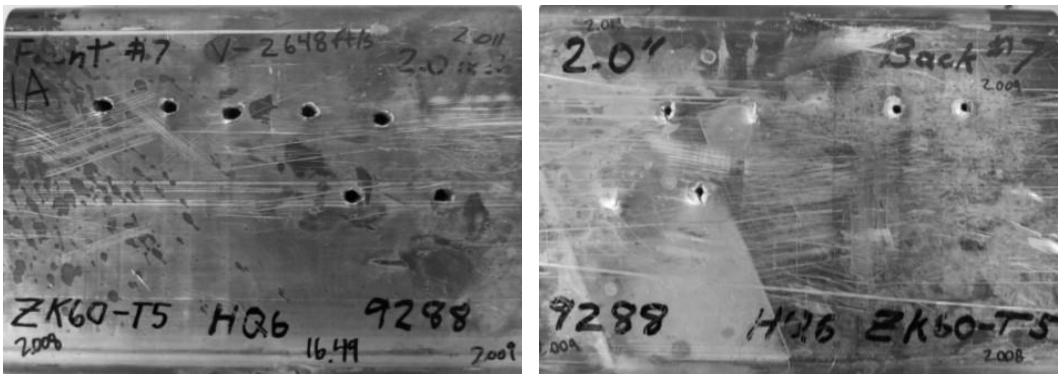

Fig. 18 ZK60A-T5 50.8-mm profile target vs. 0.30-cal. APM2, 0° obliquity, front (left) and back (right)

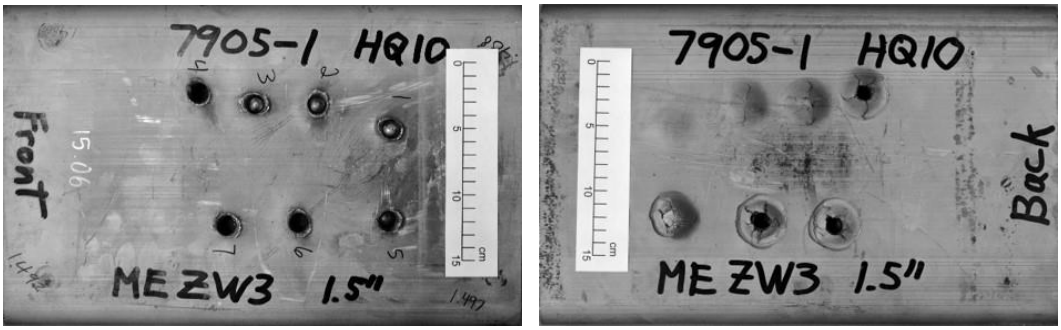

Fig. 19 ZW3 38.1-mm profile target vs. 0.50-cal. FSP, 0° obliquity, front (left) and back (right)

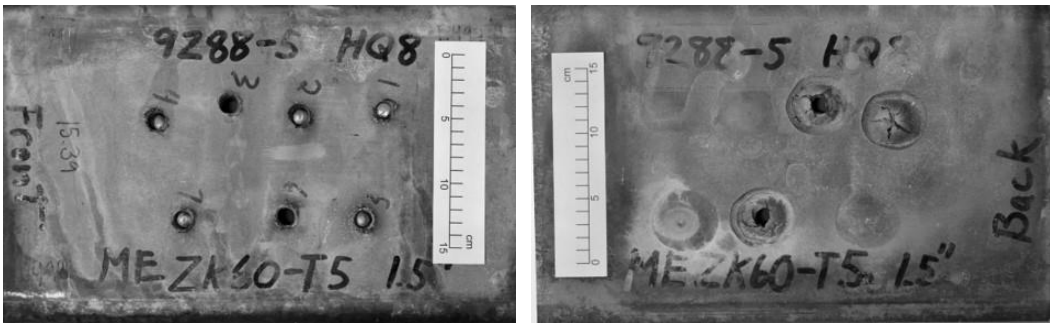

Fig. 20 ZK60A-T5 38.1-mm profile target vs. 0.50-cal. FSP, 0° obliquity, front (left) and back (right)

4.5.3 AD – V50 Regression of Test Data

Table 13 presents regression estimates of the experimental AD – V50 test performance data. Ordinarily for few or many well distributed AD versus V50 data points, a polynomial fit provides low variance in errors to performance data in comparison to the linearized exponential or logarithmic plots that may be fit with or without weight of center data points.

Table 13 Regression AD (kg/m^2) – V50 (m/s) curve fits of experimental ZW3, ZK60A-T5

Projectile, 0° Obliquity	Target Alloy	V50 Tests (n)	Polynomial Parameters, β, and the R^2 Correlation Coefficient			
			β_o	β_1	B_2	R^2
0.50-cal. FSP	ZW3	3	211.86	4.7152	0.063646	1
	ZK60A-T5	3	289.49	1.1996	0.092223	1
0.30-cal. APM2	ZW3	4	186.86	6.9714	-0.015549	0.99815
	ZK60A-T5	3	163.04	7.459	-0.016319	1

Note: V50 tests AD versus V50 data of 25.4-mm, 30.8-mm, and 50.8-mm thick targets;
Regression: Polynomial linear regression, all $V50 = \beta_o + \beta_1(AD) + \beta_2(AD)^2$

4.5.4 AD – V50 Regression Plots of Protection Levels and Comparisons

Figure 21 reveals plots of AD – V50 regression of the experimental ZW3 and ZK60A-T5 0.30-cal. APM2 ballistic test performance results, and comparisons of regression fits of reference data of Mg[12,13,14] and Al[14,15,16] AD – V50 performance. The greatest performance is with the ZK60A-T5 at the ADs near 90 kg/m^2 or 50-mm thickness, with significant performance advantages over the 5083 Al and AZ31B-H24. The plots of ZW3 and ZK60A-T5 AD – V50 regression for 0.30-cal. APM2 protection performance meet or exceed the AZ31B-H24 Mg, and 5083 Al performance. The ZK60A-T5 material appears to provide slightly higher V50 protection than the ZW3. The Al alloys 7020,[16] 7017,[17] and 7039[14,16] significantly outperform the ZW3, ZK60A-T5, and the AZ31B-H24 Mg.[12] Near AD values of 90 kg/m^2 there are minimal differences in the higher performing Mg13Li6Al, and the 7017, 7039, and 7020 Als. At V50s greater than 730 m/s, the Mg13Li6Al[14] becomes less efficient in AD. The 7020-T651 AD – V50 regression is from a limited set of all actual test data from the top 17 of 46 highest strength, or > 120 Brinell HB hardness 7020 materials.[16] The 7020 targets were obtained largely from commercial-metal distributors; therefore, custom-order melt lots with properties more specific to protection applications and with more optimal composition and purity, for properties of strength, ductility, and toughness, were not available for test and specification at the most critical test statistic thickness levels (i.e., near 40–60 mm thickness). In comparison to RHA steel[14,15] there is a small gain in performance for ADs below 60 kg/m^2, however, the performance levels remain similar over the entire range of AD.

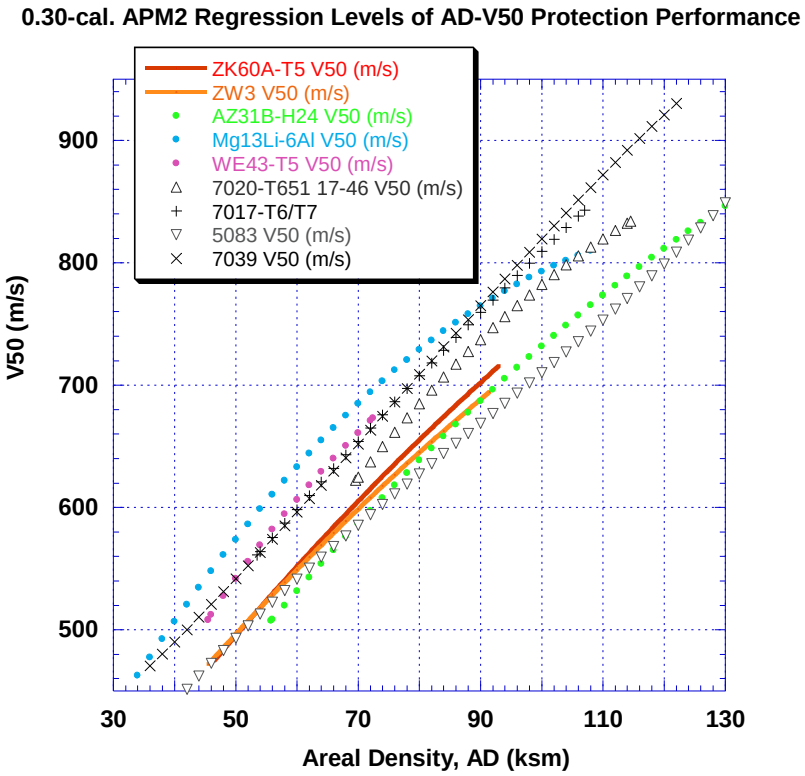

Fig. 21 Plots, AD – V50 regression, comparisons, 0.30-cal. APM2 0° obliquity protection performance

Figure 22 presents the ZW3 and ZK60A-T5 experimental material plots of 0.50-cal. FSP protection performance that are regression fit by AD – V50. The best performance is for ADs less than 56 kg/m^2 or 31 mm thickness where ZW3 or ZK60A-T5 meet performance of the high-cost WE43-T5, and significantly outperform the AZ31B-H24, and the Al protection materials; therefore, it may be assumed that ZW3 and ZK60A-T5 protection versus small fragments (e.g., 0.22-cal., and 0.30-cal. is similarly superior).[22] The plots reveal the experimental ZW3 and ZK60A-T5 protection levels are all significantly greater than Mg AZ31B-H24. With ADs greater than 50–54 kg/m^2, the AZ31-H24 Mg[12] performs poorly for fragment protection in comparison to alternative Mg ZW3 and ZK60A-T5 and the reference 7020, 7017, and 7039 Als.[14–16] For the 0.50-cal. FSP, the ZW3 material provides better protection than the ZK60A-T5, and ZW3 performs better than 5083 Al up to 63 kg/m^2 AD. The 5083 Al reference data[14,15] trends to significantly better with increasing AD than ZW3 Mg above ADs of 64 kg/m^2 or around 35 mm thickness. The lightweight AD – V50 0.50-cal. FSP performance of Mg13Li6Al[14] exceeds performance of all the alloys for 0.50-cal. FSP performance up to around 89 kg/m^2. Beginning at 54 kg/m^2 the reference data of Al alloys 7020, 7017, and 7039 protection outperforms the Mg ZW3 and 5083 Al. At 70 kg/m^2, there are minimal differences in the higher performing Mg13Li6Al, and the 7017, 7039, and

7020 Als, and the trend is for the Al alloys to outperform the Mg materials around 1,200 m/s and greater. In comparison to RHA steel[14,15] there are increasing gains in performance for ADs greater than 68 kg/m^2, and with the ZW3 the advantage is significant with a performance gain around 142 m/s at 90 kg/m^2 AD.

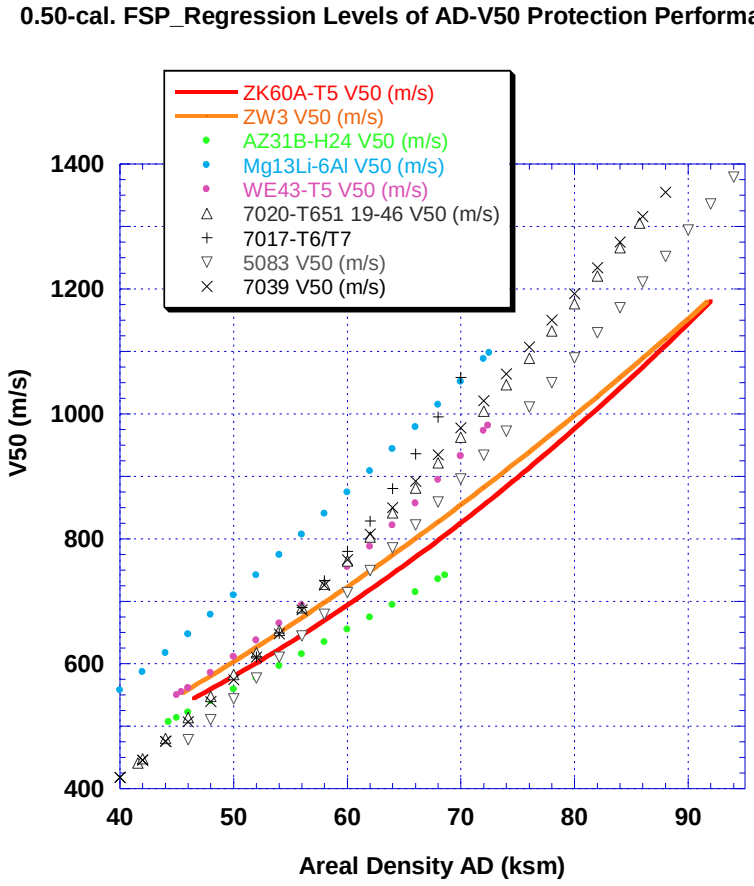

Fig. 22 Plots, AD – V50 regression, comparisons, 0.50-cal. FSP 0° obliquity protection performance

5. Conclusions

The following conclusions were reached:

1) The Zr alloy technology of the ZW3 and ZK60A demonstrate very good capability to obtain grain refinement of 50 to 100 μ during casting, and the wrought extrusion work further provides fine recrystallized grain sizes of around 10 μ.

2) The microstructure demonstrates some texture that appears as linear or non-random networks of recrystallized grains, which may make less effective

the grain refinement mechanisms of enhanced yield strength, tensile strength, and crack-toughening.

3) Charpy impact toughness energies of the ZK60A-T5 and ZW3 alloys demonstrate excellent toughness for Mg. Impact strengths in Joules exceed UN cast Charpy bars of the tough die cast AM50. Fracture features are on the size scale of the observed cast and recrystallized grain sizes.

4) Charpy UN bar impact curve analyses demonstrate near equal amounts of energy release by unstable crack fracture for ZK60A-T5 and the ZW3, with the ZW3 having less cracking and more ductile fracture. Impact curves demonstrate ZW3 with maximum force at high displacements around 5-mm followed by force reduction by ductile fracture to over 6-mm displacement, followed by final unstable crack fracture. The ZK60 impact curve demonstrates maximum force around 3-mm displacement followed by force reduction by unstable crack growth then arrest type behavior with resistance to crack growth by ductile displacement. ZW3 ductile fracture provides around 28% to 39% of the impact force reduction; ZK60A-T5 ductile fracture provides around 25% to 32% impact force reduction; the remainder of the force is reduced by unstable crack growth.

5) Impact curves of the ZW3 demonstrate excellent test time duration to sustain up to a maximum 9.5–10 kN force for 0.9 1/1000 second, followed by ductile fracture, then unstable crack growth at 1.2 1/1000 second, which is greater load and maximum force time duration than die cast Mg AM50.

6) Tensile strength of the ZK60A-T5 is equivalent to the high strength wrought AZ80 Mg alloy, and the elongation averaged 14%. The ZW3 provides lesser, near AZ80 strength but greater ductility averaging 20%. Flow curves of engineering stress versus strain demonstrate high and extended strain hardening followed by near-equal strain levels of ductile fracture.

7) Mechanical YS-TS-El properties in tension of the ZK60A-T5, which average 249-316-14, meet requirements of ASTM-B 107-13 specification. The ZW3 average mechanical properties 218-280-20 do not meet the BS 2L505 specification but meet the BS L514 extruded forging stock EFS standard for yield strength and are near the L514 standard for tensile strength.

8) The ZW3 and ZK60A-T5 density-specific Young’s modulus are equal to some but not all aluminum alloys, and are inferior to Al-Li, titanium, and many steels. Specific strengths are greater than many automotive and industrial aluminum alloys, but inferior to the highest strength industrial

aluminum, the aerospace aluminum and titanium, and the high strength and ultrahigh strength steels. Levels of specific impact toughness exceed all values for cast austempered ductile iron.

9) Ballistic impact failure modes of the 0.30-cal. APM2 projectile V50 tests demonstrate good ballistic toughness with near all ductile-hole growth. The failure modes of the targets in response to the 0.50-cal. FSP projectile are mixed mode ductile fracture followed close in the impact region with delaminating type cracks spaced through the target and with crack spall from backs of targets.

10) ZW3 and ZK60A-T5 V50 protection levels for the 0.30-cal. APM2 projectile meet or exceed performance of 5083 aluminum and AZ31B-H24 Mg. The ZK60A-T5 over the range tested, has slightly better protection; and the protection with ZK60A-T5 performs with greater advantage over 5083 Al with increasing AD. In comparison to RHA steel there is a small gain in performance for ZK60A-T5 ADs below 60 kg/m^2; however, the performance levels remain similar over the entire range of AD.

11) The V50 protection levels versus the 0.50-cal. FSP exceed and outclass AZ31B-H24 both at low and high ADs, with the ZW3 having better protection. The best performance is for ADs less than 56 kg/m^2 or 31 mm thickness where ZW3 or ZK60A-T5 meet performance of the high cost WE43-T5, and significantly outperform the AZ31B-H24, and the Al protection materials. The 0.50-cal. FSP V50 protection with ZW3 either meets or exceeds performance of 5083 aluminum up to 64 kg/m^2 or around 35-mm ZW3 thickness. High efficiencies for protection and weight saving may be attained with applications of protective shielding from small fragments. In comparison to RHA steel there are increasing gains in performance for ADs greater than 68 kg/m^2, and the advantage is significant.

12) The extruded ZW3 (ZK30) high strength and elongation experimental properties and experimental protection levels and ballistic toughness performance, the L504 standard, and the literature, suggest capability and benefits for the development of strong, Mg-tough, ZW3 plate and sheet with adequate levels of directional strength and ductility. The ZW3 appears capable of being able to be processed to Mg plate of equal or greater strength than AZ31B-H24 and to similar yield strength and ductility of aluminum 5083 and 6016, for possible useful advantages in specific strengths. The ZW3 may provide a low-cost, heat treatable, weldable plate-shape alternative, with some improved durability versus aging at

moderately elevated temperatures over the Mg-Al AM or AZ materials. In comparison to rolled WE43-T5 the ZW3 may provide plate with more uniform directional properties and improved impact toughness, crack resistance, and fracture ductility. Cast ZK61 or forged ZK60 type alloy may provide useful Mg-tough, strong, lightweight structure-shapes and components. ZW3 or ZK60 extrusions may provide lightweight, strong, tough, structural shapes for portable and prefabricated structures.

6. References

1. Luxfer MEL Technologies, Elektron wrought alloys, Datasheet: 441. Manchester (England): Luxfer MEL Technologies; 2018.
2. Friedrich HE, Mordike BL. Magnesium technology metallurgy, Design data, applications. Berlin (Germany): Springer-Verlag; 2006.
3. Polmear I. Light alloys; 4th ed.; Chapter 5 magnesium alloys; Oxford (England): Butterworth-Heinemann/Elsevier; 2006. p. 237–297.
4. Magnesium ZK60A (Heat treatable magnesium alloy), Mg-62. In: Alloy Digest. Materials Park (OH); ASM International; 1967 Apr.
5. ASTM B 107-2013. Standard specification for magnesium-alloy extruded bars, rods, shapes, tubes, and wire. West Conshohocken (PA): ASTM International; 2013.
6. Nonferrous alloys and special-purpose materials, properties of magnesium alloys. In: Housh S, Mikucki B, Stevenson A, editors. ASM Handbook: Properties and Selection. Materials Park (OH): ASM International; 1992. p. 455–516.
7. BS 2L 505: March 1973. British Standard: Aerospace series specification for bars and extruded sections of magnesium – 3% zinc-zirconium alloy. London (England): British Standards Institution; 1973.
8. EN ISO 14556:2000. Steel – Charpy V-notch pendulum impact test – instrumented test method. Dublin (Ireland): Northumberland House; 2000.
9. Dieter GE. Mechanical metallurgy. 2nd ed. New York (NY): McGraw-Hill; 1976. p. 329–377.
10. DRSTE-RP-702-101. Test operations procedure 2-2-710, AD No. A137873, Ballistic tests of armor materials. Aberdeen Proving Ground (MD): US Army Test and Evaluation Command; 1984 Feb 7.
11. MIL-STD-662F. V50 ballistic test for armor. Falls Church (VA): Defense Quality and Standardization Office; 1997 Dec.
12. Jones TL, DeLorme RD. Development of a ballistic specification for magnesium alloy AZ31B. Aberdeen Proving Ground (MD): Army Research Laboratory (US); 2008 Dec. Report No.: ARL-TR-4664.
13. Cho K, Sano T, Doherty K, Yen C, Gazonas G, Montgomery J, Moy P, Davis B, DeLorme R. Magnesium technology and manufacturing for ultra

lightweight armored ground vehicles. Aberdeen Proving Ground (MD): Army Research Laboratory (US); 2009 Feb. Report No.: ARL-RP-236.

14. Mascianica FS. Ballistic technology of lightweight armor. Watertown (MA): Army Mechanics and Materials Research Center (US); 1981 May. Report No.: AMMRC-TR 81-20.

15. Chinella JF. V50 Ballistic protection and material properties of 7020 aluminum. Aberdeen Proving Ground (MD): Army Research Laboratory (US); 2012 Sep. Report No.: ARL-TR-6148.

16. Chinella JF. 7020-T651 Aluminum properties and protection. Aberdeen Proving Ground (MD): Army Research Laboratory (US); 2017 Apr. Report No.: ARL-TR-7986.

17. Jones TL, Placzankis BE. The examination of the aluminum alloy 7017 as a replacement for the aluminum alloy 7039 in lightweight armor systems. Aberdeen Proving Ground (MD): Army Research Laboratory (US); 2016 July. Report No.: ARL-TR-7727.

18. Lyon RE, Janssens ML. Polymer flammability. San Antonio (TX): Southwest Research Institute. Washington (DC): Department of Transportation (US); 2005 May. Report No.: DOT/FAA/AR-05/14.

19. Davis AE, Robson JD, Turski M. Reducing yield asymmetry and anisotropy in wrought magnesium alloys – A comparative study, Materials Science and Engineering A. 2019;744:525–537.

20. Magnesium ZK21A: wrought magnesium alloy. In: Alloy Digest. Materials Park (OH): ASM International; 1966 June.

21. Aluminum Association. International alloy designations and chemical composition limits for wrought aluminum and wrought aluminum alloys. Standards, registration record series teal sheets, teal sheets. Arlington (VA): Aluminum Association; 2018 Aug.

22. Jones TL, Burkins MS, Delorme R, Gooch WA. Ballistic evaluation of magnesium alloy AZ31B. Aberdeen Proving Ground (MD): Army Research Laboratory (US); 2007 Apr. Report No.: ARL-TR-4077.

23. Chinella JF. Deformation and failure modes of rapidly solidified, ultra-fine grain, AMX602 and ZAXE1711 magnesium alloys. In: Manuel MV, Singh A, Alderman M, Neelameggham NR, editors. Proceedings of Magnesium Technology 2015, 144th Annual Meeting & Exhibition; 2015 Mar 15–19; Orlando, FL. Cham (Switzerland): Springer. p. 309–314.

24. Properties and selection: Irons, steels, and high-performance alloys. In: Jenkins LR, Forrest RD, editors. ASM Handbook. Materials Park (OH): ASM International, vol. 1; 1990.

25. Chinella JF, Pothier B, Wells MGH. Processing, mechanical properties, and ballistic impact effects of austempered ductile iron. Aberdeen Proving Ground (MD): Army Research Laboratory (US); 1998 Aug. Report No.: ARL-TR-1741.

26. Hammond V, Mathaudhu S, Doherty K, Walsh S, Vargas L, Placzankis B, Labukas J, Pepi M, Trexler M, Barnett B, Jones TL, Keckes L. Ultrahigh-strength magnesium alloys for the future force: a final report on the 5-year mission program, 2009-2013. Aberdeen Proving Ground (MD): Army Research Laboratory (US); 2014 Jan. Report No.: ARL-TR-6788.

27. Chinella JF, Jones TL. Evaluation of commercial aluminum alloys for armor and vehicle upgrade. Aberdeen Proving Ground (MD): Army Research Laboratory (US); 2008 Sep. Report No.: ARL-TR-4596.

28. LCOA. Alcoa automotive sheet, metal bulletin. Proceedings of the International Aluminum Conference; 2015 Sep 22; Vancouver, BC.

29. Advanz 6HS-s600 product fact sheet. Atlanta (GA): Novelis; 2019 Jan 21 [accessed 2020 Mar 10]. http://novelis.com/wp-content/uploads/2019/02/Advanz-6HS-s600-DataSheet-012119.pdf.

30. Chinella JF. High-strength Al-Cu-Li and Al-Zn alloys: mechanical properties with statistical analysis of ballistic performance. Aberdeen Proving Ground (MD): Army Research Laboratory (US); 2004 Apr. Report No.: ARL-TR-3185.

31. Uféras G. Airware 2196-T8511 extrusions. Paris (France): Constellium; 2017 May.

32. Jones TL, Burkins MS, Gooch WA. An analysis of magnesium alloy AZ31B for ballistic applications. Aberdeen Proving Ground (MD): Army Research Laboratory (US); 2007 Dec. Report No.: ARL-TR-4327.

33. TIMET. TIMETAL 6-4. Data sheet, TMC-0150. Dallas (TX): Titanium Metals Corporation; 2000.

34. EVRAZ. Armalloy 440T Armor Plate, MIL-DTL-12560J Class 4a. Specification sheet No. FP-006. 04-2015. Portland (OR): EVRAZ; 2015.

35. EVRAZ. Armalloy 500HH Armor Plate, MIL-DTL-46100E. Specification sheet No. FP-007. 04-2015. Portland (OR): EVRAZ; 2015.

36. Lewandowski JJ, Lowhaphandu P. Effects of hydrostatic pressure on deformation processing. In: effects of hydrostatic pressure on mechanical behavior and deformation processing of materials. International Materials Reviews. 1998;43(4):172–187.

Appendix A. ASTM Nomenclature of Magnesium Alloys

Table A-1 Alloy designations, select common, two-letter/two-number format ASTM B275

A	Aluminum	M	Manganese	Z	Zinc
C	Copper	Q	Silver	F	Iron
E	Rare earths	S	Silicon	N	Nickel
H	Thorium	T	Tin	V	Gadolinium
J	Strontium	W	Yttrium		
K	Zirconium	X	Calcium		
L	Lithium	Y	Yttrium		

Appendix B. Experimental Test-Note Tables and Figures

Table B-1 UN specimen, instrumented-tup (IT) Charpy impact experimental test results

Target Alloy	Profile Source	Tests (n)	A SD	Force (kN)				Displacement (mm)				Energy (J)
				F_y	F_m	F_{iu}	F_a	s_m	s_{iu}	s_a	s_t	W_t
ZW3	50.8-mm	4	A	4.50	10.00	6.07	-	4.90	5.990	-	6.15	45.88
			SD	*0.00*	*0.32*	*1.88*	-	0.19	0.27	-	0.20	1.01
	38.1-mm	3	A	4.33	10.32	8.39	2.27 [1]	4.70	5.38	[2]	6.84	45.79
			SD	*0.58*	*0.13*	*2.88*	-	0.11	0.35	[2]	1.69	2.14
	25.4-mm	2	A	4.25	10.11	7.26	-	4.59	5.93	-	6.12	47.80
			SD	*0.35*	*0.01*	*0.43*	-	0.01	0.11	-	0.06	1.00
	All	9	A	4.39	10.13	7.11	-	4.76	5.77	-	6.37	46.28
			SD	*0.33*	*0.26*	*2.14*	-	0.19	0.38	-	0.92	1.55
ZK60A -T5	50.8-mm	4	A	5.13	11.35	11.16	4.00	3.46	3.58	3.77	5.40	33.61
			SD	*0.48*	*0.16*	*1.71*	*1.01*	0.49	0.52	0.45	0.43	5.07
	38.1-mm	3	A	4.83	10.77	10.30	2.63	3.85	4.26	4.28	5.64	38.72
			SD	*0.58*	*0.62*	*0.60*	*2.28*	0.55	0.70	0.99	0.24	7.99
	25.4-mm	2	A	5.50	11.42	11.19	2.64	4.14	4.39	4.58	5.94	40.63
			SD	*0.00*	*0.15*	*0.20*	*0.13*	0.01	0.10	0.04	0.05	0.45
	All	9	A	5.11	11.17	10.88	3.24	3.74	3.99	4.12	5.60	36.87
			SD	*0.49*	*1.08*	*1.17*	*1.48*	0.50	0.62	0.67	0.36	5.98

Notes: A = Average; SD = standard deviation;
Force: F_y = yield force, approximate value, measurement not often used;
F_m = maximum force;
F_{iu} begin unstable crack propagation;
F_a = force at end of unstable crack propagation.
Displacement: s_m = displacement at maximum force;
s_{iu} = displacement at begin unstable crack propagation;
s_a = displacement at end of unstable crack propagation;
s_t = total displacement.
Energy: Wt = total energy.
1. One sample with F_a = 6.798 kN, and 2. s_a = 5.08 mm.

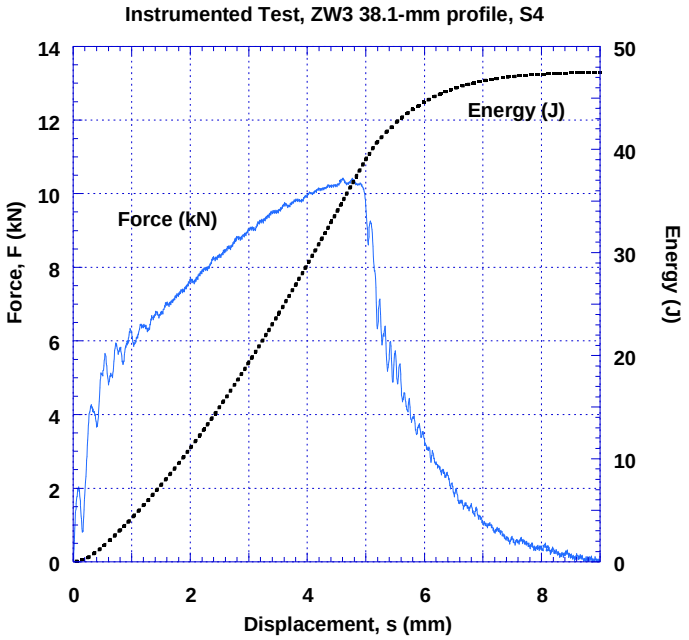

Fig. B-1 Plots, experimental Charpy IT force, energy, deflection, ZW3, LT orientation

Table B-2 Charpy instrumented test: Normalized plasticity and crack force-reduction, SDs

Target Alloy	Profile Source (mm)	Tests (n)	FRUC			PDF	Normalized Ductile Displacements			
			A	(F_{iu} - Fa) (kN)	/F_m (%)	1 - (F_{iu} - F_a)/F_m (%)	s_m s_m/s_t (%)	s_{iu} s_{iu}/s_t (%)	DF ($s_{iu} - s_m$)/s_t (%)	DCA ($s_t - s_{iu}$)/s_t (%)
ZW3	50.8	4	SD	1.9	17.7	17.7	2.2	1.5	3.5	1.5
	38.1*	3	SD	2.8	26.7	33.3	14.6	22.5	8.1	22.5
	25.4	2	SD	0.4	4.1	4.1	1.0	0.7	1.7	0.7
	All	9	SD	1.9	18.4	20.6	8.4	13.5	6.3	13.5
ZK60A-T5	50.8	4	SD	1.9	10.4	1.8	6.9	7.6	1.1	7.6
	38.1	3	SD	2.4	20.2	21.7	12.2	15.3	3.2	15.3
	25.4	2	SD	0.3	2.0	2.0	0.7	1.0	1.7	1.0
	All	9	SD	1.7	13.1	13.7	7.9	10.2	3.1	10.2

Notes:
A = Average; SD = standard deviation;
Fy = yield force; s_m = displacement at maximum force;
F_m = maximum force; s_{iu} = displacement, start of unstable crack propagation;
F_{iu} = force to begin unstable crack propagation; s_a = displacement at end of unstable crack propagation;
Fa = force at end of unstable crack propagation; s_t = total displacement;
FRUC = force reduction by unstable crack extension, absolute ($F_{iu} - F_a$), normalized ($F_{iu} - Fa)/F_m$;
PDF = Proportion of ductile fracture surface (C.1 of ISO 14556: 2000)
s_m/s_t = ductile displacement to maximum load normalized to total displacement (NTTD, Sm/St;
s_{iu}/s_t = ductile displacement to initiation of fracture NTTD, Siu/St;
DF = ductile displacement by plastic fracture prior to unstable crack extension NTTD, (Siu – Sm)/St;
DCA = extent of ductile displacement by crack arrest resistance to crack propagation NTTD, (St – Siu)/St.

Table B-3 Experimental engineering stress and strain in tension, ZW3, ZK60A-T5, SDs

Alloy	Profile	No. Specs.	YM (GPa)	YM (Msi)	YS (MPa)	YS (ksi)	TS (MPa)	TS (ksi)	El (%)	RA (%)	TS-YS (MPa)	YS/TS
ZW3	25.4	2	2.5	0.4	3.6	0.5	0.1	0.0	3.7	1.5	3.5	0.01
	38.1	2	0.8	0.1	4.3	0.6	4.9	0.7	0.0	3.9	0.6	0.00
	50.8	3	3.5	0.5	5.8	0.8	6.1	0.9	1.0	2.7	0.4	0.00
	All	7	2.5	0.4	8.3	1.2	6.4	0.9	1.7	4.4	2.6	0.01
ZK60A	25.4	2	3.7	0.5	2.2	0.3	0.9	0.1	0.3	4.7	1.3	0.00
	38.1	2	3.3	0.5	8.1	1.2	14.1	2.0	1.5	2.5	6.0	0.01
	50.8	3	4.5	0.7	6.6	1.0	5.0	0.7	0.5	3.7	2.9	0.01
	All	7	3.4	0.5	7.8	1.1	6.8	1.0	0.8	3.2	4.7	0.01

Notes: SD = standard deviation

Table B-4 Experimental true stress and strain in tension, ZW3, ZK60A-T5, SDs

Alloy			True: stress σ, strain ε					Flow curve $\sigma = K\varepsilon^n$	
Alloy	Profile	No. Specs.	TUσ (MPa)	TUε	TLNε	TFσ (MPa)	TFε	n	K (MPa)
ZW3	25.4	2	1.1	0.00	0.02	21.2	0.02	0.003	2.9
	38.1	2	4.9	0.00	0.06	20.0	0.06	0.005	2.1
	50.8	3	6.7	0.00	0.04	6.3	0.04	0.002	8.7
	All	7	7.0	0.00	0.06	19.0	0.06	0.005	7.0
ZK60A	25.4	2	1.6	0.00	0.06	15.8	0.06	0.002	3.5
	38.1	2	16.9	0.01	0.03	31.1	0.03	0.002	16.6
	50.8	3	5.5	0.00	0.05	5.4	0.05	0.002	5.2
		7	7.9	0.00	0.04	15.3	0.04	0.004	7.8

Notes: Totals, ZW3 YS = 31.6 (ksi), TS = 40.6 (ksi);
ZK60A-T5 YS = 36.1 (ksi), TS = 45.8 (ksi);
SD = standard deviation

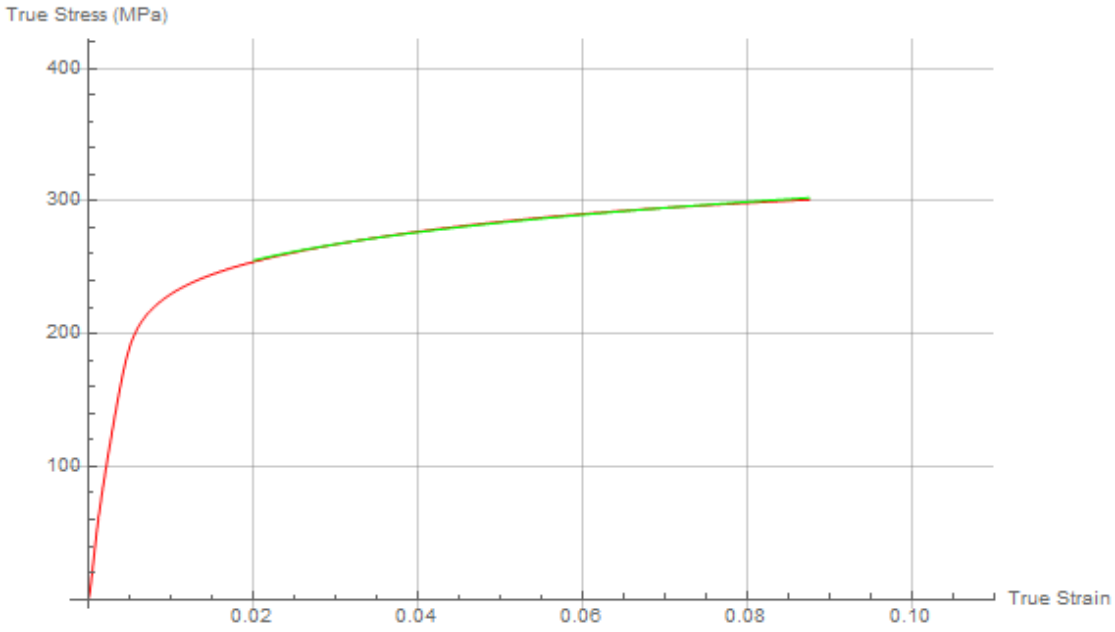

Fig. B-2 Flow curves of true stress vs. true strain to (σ_u, ε_u) (red), and power law fit $\sigma = K\varepsilon^n$ from 0.02 ε to (σ_u, ε_u), (green)

List of Symbols, Abbreviations, and Acronyms

ABRC	alternate biaxial reverse corrugation
AD	areal density
ADI	austempered ductile iron
Al	aluminum
ASTM	American Society of Testing Materials
BSI	British Standard Institution
Ca	calcium
Ce	cerium
CP	complete penetration
Cu	copper
DF	ductile fracture
DIC	digital image correlation
EFS	Extruded Forging Stock
El	elongation
F	force
Fe	iron
FRUC	force reduction by unstable crack growth
FSP	fragment-simulating projectile
HCP	hexagonal close packed
HRE	Rockwell E hardness
IT	instrumented test
K	potassium
L	longitudinal
La	lanthanum
Li	lithium
Mg	magnesium

Mn	manganese
Na	sodium
Nd	neodymium
Ni	nickel
NTS	National Technical Systems
OM	optical microscopy
PDF	proportion of ductile fracture surface
PP	partial penetration
Pr	praseodymium
RA	reduction of area
RD	rolling direction
RE	rare earth
RHA	rolled homogeneous armor
RLC	rolled low-cost
SD	standard deviations
STA	solution treated and aged
SWAP	Spinning Water Atomization Process
TS	tensile strength
UN	un-notched
Y	yttrium
YS	yield strength
Zn	zinc
Zr	zirconium

1 (PDF) DEFENSE TECHNICAL INFORMATION CTR DTIC OCA

1 (PDF) CCDC ARL FCDD RLD CL TECH LIB

1 (PDF) CCDC ARL FCDD RLW MF J CHINELLA